T.C.

GEBZE YÜKSEK TEKNOLOJİ ENSTİTÜSÜ

MÜHENDİSLİK VE FEN BİLİMLERİ ENSTİTÜSÜ

RASTGELE OLMAYAN İKİ ELEKTROLİT SIVI (ENRTL) MODELİ İLE POTASYUM KARBONAT ERİYİĞİNDE KARBON DİOKSİT ÇÖZÜNÜRLÜĞÜ HESAPLANMASI

YAN PROVINTA LAKSANA

YÜKSEK LİSANS TEZİ

KİMYA MÜHENDİSLİĞİ

ANA BİLİM DALI

GEBZE

2012

T.C.

GEBZE YÜKSEK TEKNOLOJİ ENSTİTÜSÜ

MÜHENDİSLİK VE FEN BİLİMLERİ ENSTİTÜSÜ

RASTGELE OLMAYAN İKİ ELEKTROLİT SIVI (ENRTL) MODELİ İLE POTASYUM KARBONAT ERİYİĞİNDE KARBON DİOKSİT ÇÖZÜNÜRLÜĞÜ HESAPLANMASI

YAN PROVINTA LAKSANA

YÜKSEK LİSANS TEZİ

KİMYA MÜHENDİSLİĞİ

ANA BİLİM DALI

TEZ DANISMANI

Prof. Dr. Mehmet Alaittin HASTAOĞLU

GEBZE

2012

YÜKSEK LİSANS TEZİ JÜRİ ONAY SAYFASI

G.Y.T.E. Mühendislik ve Fen Bilimleri Enstitüsü Yönetim Kurulu'nun 11.06.2012 tarih ve 2012/23..... sayılı kararıyla oluşturulan jüri tarafından 12.06.2012.. tarihinde tez savunma sınavı yapılan Yan Proviınta Laksana'ın tez çalışması Kimya Mühendisliği Anabilim Dalında YÜKSEK LİSANS tezi olarak kabul edilmiştir.

JÜRİ

ÜYE (TEZ DANIŞMANI)	:	Prof. Dr. Mehmet Alaittin HASTAOĞLU	MAHastaoglu
ÜYE	:	Prof. Dr. Murat ÖZDEMİR	M. Özdemir
ÜYE	:	Yrd. Doç. Dr. Tunahan ÇAKIR	TÇ

ONAY

G.Y.T.E. Mühendislik ve Fen Bilimleri Enstitüsü Yönetim Kurulu'nun ...../...../20... tarih ve ...../..... sayılı kararı.

İMZA/MÜHÜR

ÖZET

TEZ BAŞLIĞI : Rastgele Olmayan İki Elektrolit Sıvı (ENRTL) Modeli İle Potasyum Karbonat Eriyiğinde Karbondioksit Çözünürlüğü Hesaplanması

YAZAR ADI : Yan Provinta Laksana

MATLAB programı kullanarak Rastgele Olmayan İki Elektrolit Sıvı (ENRTL) aktivite katsayısı modeli ile, potasyum karbonat-solvent-elektrolit sisteminde karbondioksit çözünürlüğü hesaplanmıştır. Bu veriler endüstriyel uygulama olarak baca gazı temizlemesi veya amonyak üretimi için yararlı olur. Model karbondioksitin çözünürlüğünü konsantrasyon ve sıcaklığın fonksiyonu olarak tahmin etmekte, böylece buhar-sıvı dengesinde K_2CO_3-H_2O-CO_2 sistemi için termodinamik veriler sağlamaktadır. Literatürden alınan parametreler kullanılarak MATLAB'ta Pitzer-Debye-Hückel (PDH), Born, ve yoresel katkısı denklemi uygulayarak karbondioksit çözünürlüğü için deneysel verilere benzer eğilimler bulunmuştur. Sabit basınçta, ortalama bağıl sapma %5 ile %12 arasında bulunmuştur, ki bu da deney sonuçlarıyla olumlu olarak kıyaslanmıştır. Ayrıca, solvent konsantrasyonu ve sıcaklığın karbondioksit çözünürlüğüne etkisi vardır. Yüksek solvent konsantrasyonu ve çalışma sıcaklığı karbondioksit elektrolit sistemlerinde çözünürlüğü arttırmıştır.

Anahtar kelimeler: Absorpsiyon, çözünürlük, Rastgele-Olmayan-İki-Elektrolit-Sıvı (ENRTL), H_2O-K_2CO_3-CO_2.

SUMMARY

TITLE OF THESIS : Prediction of Carbon Dioxide Solubility in Potassium Carbonate Aqueous Solution with Electrolyte Non Random Two Liquid (ENRTL) Model

AUTHOR : Yan Provinta Laksana

The Electrolyte-Non-Random-Two-Liquid (ENRTL) activity coefficient model implemented in MATLAB was used to predict carbon dioxide solubility in aqueous potassium carbonate-solvent-electrolyte system for the application of carbon dioxide absorption or removal in industrial case such as flue gas and ammonia production. The model predicts solubility of carbon dioxide as a function of solvent concentration and operating temperature to provide thermodynamic data especially vapor-liquid equilibrium for K_2CO_3-H_2O-CO_2 system at industrial application for CO_2 absorption with potassium carbonate solution. Using parameters from the literature and applying equation of Pitzer-Debye-Hückel, Born, and local contribution of ion in MATLAB software resulted in similar trends for CO_2 solubility correlating the experimental data. For the constant pressure, average relative deviation obtained ranged from 5% to 12% which compared satisfactorily to the experimental data. In addition, solvent concentration and temperature had impact on CO_2 solubility. The higher concentration of solvent and operating temperature increased CO_2 solubility in the electrolyte systems.

Keywords : Absorption, solubility, Electrolyte-Non-Random-Two-Liquid (ENRTL),K_2CO_3-H_2O-CO_2.

ACKNOWLEDGEMENTS

The author initially wish to thank to Allah for life and healthiness so far that the author could finish studying in Gebze Institute of Technology, Turkiye and writing the thesis as partial fulfillment the requirements of Master Degree in Chemical Engineering.

The author also sincerely likes to thank thesis advisor Prof. Dr. Mehmet Alaittin HASTAOĞLU for all the support, guidance, and mentorship over the course of the thesis. He gave the author advice to build a structural scientific writing and whenever the author made wrong direction he always helped the author return to right track. He not only encourages the author to explore many ideas but also give assistance to solve any problems even for non academic case. The author is very grateful.

The author likes to thank to thesis committee member Prof. Dr. Murat ÖZDEMİR and Yrd. Doç. Dr. Tunahan ÇAKIR for their valuable suggestion and advice. Certainly, author would also thank to all academic member of Chemical Engineering Department Gebze Institute of Technology for their support.

Thanks to author's family, though they couldn't present to academic process in Turkiye but their support and praying always make the author believe that they always close. Finally, author wish to thank for all author's friend this time. They are ready to share happiness and sorrow during author stays in Turkiye.

TABLE OF CONTENTS

LIST OF FIGURES

LIST OF TABLES

CHAPTER I

INTRODUCTION

1. 1 Background

Removal of acidic gases such as carbon dioxide is one of important industrial applications. Carbon dioxide can either be produced in industries or occur naturally in oil and gas production. The main reason to remove carbon dioxide content is due to technical and economical concerns. Carbon dioxide present in natural gas reduces the heating value of gas and as part of acidic gases; it also has potential to corrode material in pipe and process equipment. Also carbon dioxide poisons catalyst in ammonia synthesis (Othmer, 2005). Natural gas pipelines usually allow CO_2 concentrations from 1 to 2% in mole. In the past decade, CO_2 removal from flue gas stream started as a potentially economic source mainly for Enhanced Oil Recovery (EOR). Moreover, CO_2 was produced to supply industrial applications such as welding as inert gas, food and beverage carbonation, urea production, dry ice, and soda-ash industries (Othmer, 2005). However, environmental concerns, especially in global climate change, have motivated scientific research in sequestration and capture of CO_2. Carbon dioxide is considered as Green House Effect (GHE) gas which is responsible for global climate change in addition to methane, nitrous oxide, and some industrial gases. Scientific research has demonstrated that increasing GHE gases can lead to increase of temperature of Earth's surface and change global climate.

A wide range of separation and capture techniques for CO_2 has been developed. Separation of CO_2 from other gases such as natural gas or biomass conversion can be done in a variety of ways involving several separation steps. If that the gas is assumed to consist of carbon, hydrogen, oxygen, and some inert compounds as an input stream, there are several paths for separating a concentrated stream of CO_2 such as membranes, cryogenic (separation of gas by condensation), adsorption, and chemical absorption By using membranes, it is difficult to achieve high purity, concentrated CO_2 stream, particularly on the scale of CO_2 capture from power plant. Cryogenic separation is a reliable process producing a high pressure and

liquid CO_2 stream; however this CO_2 sequestration requires high cost because of refrigeration

and water removal process. Otherwise water will form a solid content and possibly disrupt the separation. Cryogenic technology is usually only considered for highly concentrated CO_2 streams. Adsorption has been tested but a low capacity and poor CO_2 selectivity limit the potential for CO_2 capture. Absorption methods can be a good option to remove CO_2 especially for CO_2 gas streams with low concentrations. In addition, it is quite easy to regenerate the absorbents after absorbing CO_2 in the process. Some improvement is being developed to achieve higher efficiency of chemical absorption.

1.2 Chemical Absorption

The most common technology to remove low concentration CO_2 is absorption with chemical solvents. This chemical absorption is adapted from the gas processing industry where amine based processes have been used commercially for removal of acid gas impurities from process gas stream. However, problems of scale, efficiency, and stability become barriers when chemical solvents are used for high-volume gas flows with relatively smaller fraction of valuable product. The processes require large amount of material undergoing significant changes in conditions, leading to high investment cost and energy consumption. In addition, degradation and oxidation of solvent over time produces corrosive components needing attention to handle hazardous material procedures (Astarita et al. 1983).

In the most common absorption process (Fig. 1.1) with the temperature swing variation, a waste gas containing CO_2 enters the bottom of an absorber. The CO_2 is removed and the treated gas exits to the top of the column. A carbon dioxide-lean solvent enters the top of the absorber and counter currently contacts the gas phase in packings or trays. CO_2 is absorbed and the rich solvent exits the absorber. The rich solvent then is pre-heated in a cross heat exchanger and pumped to the top of a stripper. Heat, from low or intermediate pressure steam, is applied to regenerate the solvent and concentrated CO_2 is recovered. Some heat is recovered from the lean-solvent though the solvent requires further cooling before its re-use in the absorber.

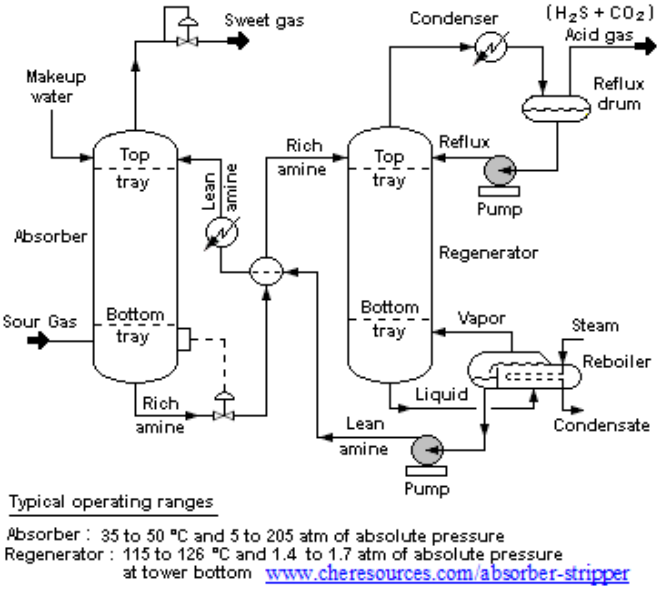

Figure 1.1 Absorber-Stripper Solvent Columns.

A variety conditions is encountered depending on the specification of the process. Table 1.1 shows some constraints specific to the most common CO_2 removal application and the potential conditions for removal in the power plant setting (Othmer, 2005).

Table 1.1 Process Condition in Absorber/Stripper for CO_2 Capture.

Process	Inlet CO_2 % vol	Outlet CO_2 % vol	P_{tot} Atm
Natural Gas	0 - 50	1 - 2	10 - 70
Ammonia	17 - 19	0.01 - 0.2	30
Coal Power Plant	10 -15	1 - 1.5	1 - 1.3
Natural Gas Power Plant	2 - 3	0.2 - 0.3	1 - 1.3

1.2.1 Process Description

The application of carbon dioxide absorption firstly was introduced by Benson *et al.* (1954) by using hot potassium carbonate to remove carbon dioxide in gas synthesis. Synthesis gas then was applied for Fischer-Trops process at high pressures, hence the absorption was held with hot and concentrated alkaline solutions of potassium carbonate within range of high pressure. The process of absorption was meant for further application such as pressurized combustion and reforming

processes. It was initial step to study chemical absorption with hot alkaline solution and higher pressure (Chapel and Ernst, 1999).

The absorption process studied by Benson et al. (1954) also found that the chemical reaction of potassium carbonate while absorbing carbon dioxide was forming potassium bicarbonate. Therefore, absorption near 120°C was prohibitive since it was boiling point of the solution and conversion of bicarbonate could only reach 35%. The use of 50% solution was also applied but it had not given better result because the boiling point of solution was decreasing into 113°C though the conversion of reaction between potassium carbonate and carbon dioxide was increased exceeds 48%. Instead of previous process, application of 40% solution indicated best process result. The conversion achieved 90% with 107°C of boiling point, henceforth the solution was employed at 40-45% to give better performance of absorption.

The absorption of carbon dioxide by using potassium carbonate can be described in the figure 1.1. Industrial applications generally operate high pressure of absorber (more than 10 atm). In high pressure, the driving force for CO2 transfer from gas phase into liquid phase is occured. In addition, the process work at high temperatures (within 100°C) and the desorption process also utilize the same condition as the absorption. The flue gas feeded in lower temperature before entering the desorber can be carried by using hot potassium carbonate exiting the desorber in cross-heat exchanger. When solution enters the desorber, it then flashes and releases dissolved CO2 to produce cooler solution. The steam is needed to provide constant operating temperature and generate sensible heat for the solution. However, for potassium carbonate system steam requirement is lower than in amine system since the sensible heat of potassium carbonate is lower than amine solution such as monoethanolamine (MEA) resulting more effective process in steam consumption (Chapel and Ernst, 1999).

The solvent losses in gas out from the absorber can be minimized since potassium carbonate solution is not volatile compound. It is known also that potassium carbonate tends to keep equilibrium reaction longer with presence of MEA, the process of mixed solution gives near no loss solvent.

1.2.2 Chemistry of the Potassium Carbonate System

The reaction in absorption process for carbon dioxide removal by potassium carbonate solution can be written below

$$CO_2 + K_2CO_3 + H_2O \leftrightarrow 2KHCO_3 \quad (1.1)$$

Both of potassium carbonate and potassium bicarbonate are classified as strong electrolyte solution, the ionic reaction can be presented as

$$CO_2 + CO_3^{2-} + H_2O \leftrightarrow 2HCO_3^- \quad (1.2)$$

As shown in reaction (1.2), trimolecular reaction occurs and the reaction can be represented in some elementary steps. The elementary reactions of carbon dioxide absorption is employed with bicarbonate production:

$$CO_2 + 2H_2O \leftrightarrow HCO_3^- + H_3O^+ \quad (1.3)$$

$$CO_3^{2-} + H_3O^+ \leftrightarrow HCO_3^- + H_2O \quad (1.4)$$

Reaction (1.3) and (1.4) also bring together with dissociation of water as shown below:

$$2H_2O \leftrightarrow H_3O^+ + OH^- \quad (1.5)$$

The overall chemical reactions are Eqs. (1.3)-(1.5). Reactions (1.4) and (1.5) are instantaneous reactions and it is reaction (1.3) that control the step for absorption of CO_3 (Reddy et al. 2003).

The equilibrium constant of the reactions are dependence with temperature and able to be calculated as:

$$\ln K_x = A + \frac{B}{T} + C\ln T + DT \quad (1.6)$$

The parameters A, B, C, and D are taken from Prausnitz et. al. (1999) and shown in Table 1.2.

Table 1.2 Equilibrium constant parameters for K_2CO_3 system.

Reaction	A	B	C	D
$CO_2 + 2H_2O \leftrightarrow H_3O^+ + HCO_3^-$	231.465	-12092.1	-36.7816	0
$HCO_3^- + H_2O \leftrightarrow CO_3^{2-} + H_3O^+$	216.050	-12431.7	-35.4819	0

1.2.3 Process Efficiency and Cost

While CO_2 absorption has been proposed for power plant application, the cost of technology is currently high. Estimations suggest an 80% increase in the cost for electricity from coal fired power plants with CO_2 capture. The components of this cost must be understood to effectively improve upon the process and move towards commercialization. The capture and compression of CO_2 accounts for 80% of the total cost and the balance (20%) is due to transportation and sequestration. The obvious obstacle for implementation is the capture of CO_2, therefore a significant opportunity for reducing cost lies with improving the capture process (Rao and Rubin, 2002).

Within the capture process, compression accounts for 34% of the cost (Rao and Rubin, 2002). The efficiency of this component will be dictated by pressure and temperature of the concentrated gas stream. Approximately 17% of the total operating cost is from circulation of the solvent and gas through the column by pumps and blowers. Minimizing pressure drop and consequently packing height may be a consideration in reducing the cost. Rao and Rubin (2002) also reported that the most significant cost of CO_2 capture is the energy requirement of solvent regeneration, up to 49% of the total capture cost. The regeneration energy required can be estimated from solvent properties. The following solvent properties may cause the most significant factor in determining the cost regeneration.

The solvent capacity is a measure of the CO_2 amount absorbed per unit quantity of the solvent. The capacity defines the total CO_2 concentration change over a set range of equilibrium partial pressure, reflecting the vapor-liquid equilibrium characteristics of a solvent. A high solvent capacity indicates that more CO_2 can be absorbed or stripped with a set amount of energy. Thus, given a constant circulation rate, the process becomes more efficient.

The heat of CO_2 absorption is another important property. As CO_2 reacts with the solvent in the absorber, heat is liberated. Excluding latent and sensible heats, an amount of heat equivalent to this must be applied to reverse the reaction and remove CO_2 from the solution in the stripper. The application of this property to energy assessments is straightforward in that reduction ordinarily lowers the required energy per mol of CO_2.

Improving the rate of CO_2 absorption into a solvent impacts several facets of the process and provides additional process flexibility. A faster rate of absorption for a given separation allows the reduction of the liquid flow rate or reduction in packing height. It can save costs associated with liquid holdup, pressure drop, and latent heat. Alternatively the absorber can be run closer to the equilibrium, which may be the more favorable option depending on the solvent capacity (Bartoo, 1984).

The currently preferred solvent solution to separate CO_2 in industrial application is amine-based chemical absorbents. Sholeh (2005) studied that carbon dioxide in the gas phase could dissolve into solution of water and amine compound. Mono ethanolamine (MEA) is inexpensive and the lowest molecular weight of amine compounds, it has been used mainly for separation of CO_2 in natural gas stream. MEA has a high enthalpy of solution with CO_2, which tends to drive the dissolution process at high rates. However, this also means that a significant amount must be used for regeneration. In addition, high vapor pressure and irreversible reactions with minor impurities such as COS and CS_4 can result in solvent loss.

Research on improved chemical solvents is looking for a high absorption capacity for CO_2 without a corresponding large energy requirement for regeneration. Other desirable properties include high chemical stability, low vapor pressure, and low corrosiveness. It has been shown also by Cullinane and Rochelle (2004) that solvent based piperazine (PZ)-promoted K_2CO_3 can have reaction rate approaching MEA but currently with lower capacity. Sterically hindered amines have been developed with similar capacity and possibly less energy requirement for regeneration than conventional MEA absorbent. These modified amines attempt to balance good absorption and regeneration characteristics under some conditions due to reduced chemical stability of the amine-CO_2 anion. Controlled species selectivity is also possible with these compounds.

1.3 Previous Studies

Tosh et al. (1959) investigated the equilibrium behavior of the K_2CO_3-CO_2-H_2O system in some variables. There were temperature range from 343 to 413 K and K_2CO_3 percentage weight concentrations 20, 30, and 40%. Flash calculations were done in ASPEN simulation by Anusha (2010). Calculations were performed for constant weight solution at 40% of K_2CO_3 at temperatures of 70, 90, 110, and 130ºC. The calculations between Tosh et al. (1959) and Anusha (2010) then were compared.

Anusha (2010) has resulted deviation from the ASPEN simulation compared to experimental results. The deviation occured particularly at higher temperatures and loading of CO2. The higher temperature should be paid attention since in the 40% weight base solution the boiling point of potassium carbonate is near 110°C.

Cullinane (2005) and Hilliard (2004) have performed the utilisation of VLE (Vapor-Liquid-Equilibrium) of the system with the Electrolyte-Non-Random-Two-Liquid (ENRTL) model and regressed the values for the temperature dependent interaction parameters. In his study, Cullinane (2005) only used VLE data from Tosh et al. (1959) to apply regression for parameters. This may not give precise an accurate representation for the interactions in the system since experimental errors can be taken place significantly in the VLE measurements. However, Hilliard (2004) used data from a number of sources to regress the values of the interaction parameters, particularly data from Aseyev and Zaytsev (1996) for H_2O-K_2CO_3 system with temperature range of 298 to 403 K and 14 to 50 wt.% K_2CO_3 solution and for H_2O-$KHCO_3$ system with temperature range of 278 to 403 K. Hilliard (2004) also employed data from Tosh et al. (1959) to find better regression of VLE measurements for K_2CO_3-H_2O-CO_2 system. Thus, utilizing the modified parameters gives a much better representation of the VLE of the system and these parameters were used in the rest of analyses.

1.4 Objective and Scope

The objective of this thesis is to determine the solubility range of CO_2 in potassium carbonate solution and to model the vapor-liquid equilibrium system in order to model the absorption process better. Data obtained from this work then can be used in the design of absorber and stripper system.

Solubility of CO_2 in potassium carbonate is part of required data to build vapor-liquid equilibrium (VLE) chart and then the VLE chart is basic information for designing CO_2 absorber-stripper system using potassium carbonate as chemical absorber. Electrolyte Non Random Two Liquid (ENRTL) model is choosed since it gives better ionic activity in electrolyte solution.

To build VLE chart, it is needed to gather solubility data in some variables condition particularly pressure, temperature, and mass fraction of solution. In this work pressure condition is maintained in 1 atm as for temperature and mass fraction vary in range 30 - 90° Celsius and 20-40% mass fraction of potassium carbonate solution.

CHAPTER 2

LITERATURE REVIEW

2.1 Thermodynamic Equilibrium Phase

Equilibrium between phases in thermodynamic scale can include vapor liquid equilibrium (VLE), liquid-liquid equilibrium (LLE), and solid-vapor equilibrium (SVE). These describe that one phase is said to be equilibrium if providing equal state with the other phase (Smith et al. 1996). The characteristics of phase equilibrium in thermodynamic term is appearance of fugacity, pressure, and temperature equality for each component in any phase that can be written as

$$f^{v} = f^{l} \tag{2.1}$$

Lewis-Randall rule describes the definition of fugacity for ideal solution as a function of concentration.

$$f^{ideal} = x_i f_i \tag{2.2}$$

where x_i is mol fraction of species i. For nonideal solutions a correction factor will be needed to define activity coefficient, γ

$$\gamma_i = \frac{f_i}{f^{ideal}} = \frac{f_i}{x_i f_i} \tag{2.3}$$

The concept of fugacity was introduced for real gases to obtain a simple relation for the chemical potential analogous to the ideal gases. At constant temperature, this relation for the chemical potential can be expressed as

$$\mu_i = \mu_i^{\circ} + \int_{P^{\circ}}^{P} v_i \, dP \tag{2.4}$$

Substituting the ideal gas equation

$$v_i = \frac{RT}{P} \tag{2.5}$$

and integrating Eq. (2.4) from the standard pressure P° to the system pressure P gives the final expression for the chemical potential at temperature T and pressure P:

$$\mu_i - \mu_i^o = RT \ln \frac{P}{P^o} \qquad (2.6)$$

Equation (2.6) shows the change in the abstract thermodynamic quantity μ as a simple logarithmic function of physical real quantity, pressure. However this relation is valid only for pure, ideal gases. To obtain a broader application, the fugacity must be introduced instead of pressure for a mixed system (Ellies, 1959).

Equilibrium condition can be defined with Gibbs energy, G, in the system. The change of Gibbs energy for irreversible system obeys the following inequality

$$dG^{tot} \leq 0 \qquad (2.7)$$

The inequality above represents that if we work at closed system with constant pressure and temperature, when any other property changes will decrease total Gibbs energy, G. In other words G reaches minimum values while system is in equilibrium condition (Smith et al. 1996).

In aqueous solutions, volatile electrolytes exist in ionic and molecular forms. At ordinary temperature and pressure, only the molecular form exists in the vapor phase. The CO_2-alkanolamine-water system is one of the examples of weak electrolyte reactive systems. When CO_2 is absorbed into an alkanolamine solution, the chemical reactions result in a complex mixture of volatile molecular species and non volatile ionic species. Calculation of VLE requires simultaneous solution of phase-equilibrium equations for the molecular species, chemical equilibrium equations for the liquid phase, and material balances. The coupling between phase and chemical equilibrium is schematically illustrated in Figure 2.1 (Edwards et al. 1975).

In terms of a thermodynamic model especially for estimation of equilibrium system, we need also to develop equilibrium representation of a complex chemical solution in a closed system. For example, Cullinane and Rochelle (2004) used K+/Piperazine (PZ) mixtures. Several chemical reactions can occur as shown below since all of the species in solution react. Temperature and nominal solution composition are properties that can change the equilibrium concentrations:

$$CO_2(g) \leftrightarrow CO_2(aq) \quad (2.8)$$

$$H_2O(g) \leftrightarrow H_2O(aq) \quad (2.9)$$

$$CO_2(aq) + 2H_2O \leftrightarrow HCO_3^- + H_3O^+ \quad (2.10)$$

$$HCO_3^- + H_2O \leftrightarrow CO_3^{2-} + H_3O^+ \quad (2.11)$$

$$2H_2O \leftrightarrow H_3O^+ + OH^- \quad (2.12)$$

$$PZH^+ + H_2O \leftrightarrow PZ(l) + H_3O^+ \quad (2.13)$$

$$PZ(l) + CO_2\,(aq) + H_2O \leftrightarrow PZCOO^- + H_3O^+ \quad (2.14)$$

$$H^+PZCOO^- + H_2O \leftrightarrow PZCOO^- + H_3O^+ \quad (2.15)$$

$$PZCOO^- + CO_2 + H_2O \leftrightarrow PZ(COO^-)_2 + H_3O^+ \quad (2.16)$$

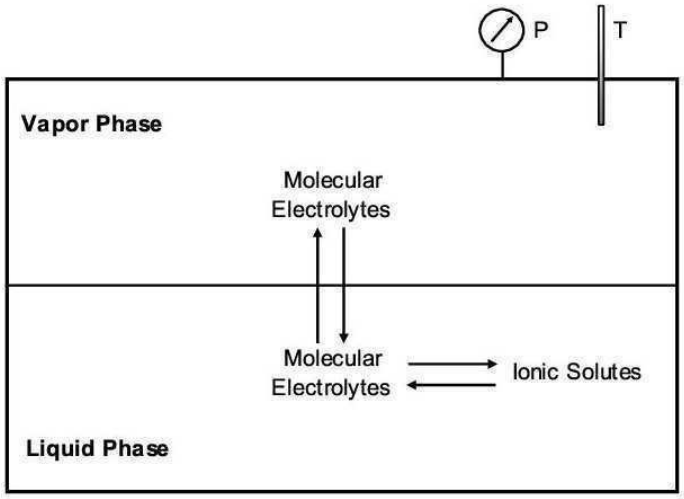

Figure 2.1 Schematic representation of vapor-liquid equilibrium for an aqueous weak electrolyte solution

The problem for calculation of equilibrium compositions which is defined by these reactions is easily known if the macroscopic properties of mixtures have been presented. The properties to be presented covers total concentrations of K+ and PZ, and temperature.

In addition, to give rigorous equilibrium system the calculation of non ideal variables that occurs at reactions above should be presented as rigorous solution.

2.2 Chemical Equilibrium and Excess Gibbs Energy

A closed homogenous system is one with uniform properties throughout without exchanging matter inside the system with its surrounding, although it may exchange energy. The number of moles of each species in a closed system not undergoing chemical reaction is constant. A thermodynamic equilibrium is reached when interactions of the system with its surroundings in the form of heat transfer and work of volumetric displacement is reversible at a constant temperature and pressure. The general condition of thermodynamic equilibrium can then be written as a combined statement of the first and second laws of thermodynamics (Prausnitz et al, 1999).

$$dU = TdS - PdV \tag{2.17}$$

where dU, dS, and dV are respectively small changes in internal energy, entropy, and volume of the system respectively. The first term on the right (TdS) is the heat absorbed by the system and the second term (PdV) is the work done by the system. Entropy, S, and volume, V, are independent variables for the system.

By interchanging both T and S then P and V in Eq. (2.17) above so as to use T and P as the independent variables, Gibbs free energy, G, is then defined as

$$G \equiv U - TS - (-PV) \tag{2.18}$$

which gives

$$dG = - SdT + VdP \tag{2.19}$$

in which at constant T and P indicated as subscripts, Eq. (2.19) reduces to:

$$(dG)_{T,P} = 0 \tag{2.20}$$

Equation (2.20) shows the thermodynamic equilibrium condition for a closed homogenous system at constant T and P in which Gibbs free energy reaches its minimum.

Consider a closed heterogeneous system, made up of two or more phases where each phase is treated as an open system within the overall closed system. There is mass and heat transfer between the various phases in the system. At thermal and mechanical equilibrium, temperature and pressure are uniform throughout the entire heterogeneous closed system in which surface forces, semipermeable membranes, and electric, magnetic, or gravitational forces is not considered. These conditions of phase equilibrium for the heterogeneous closed system consisting of π phases and N components can be summarized as follows:

$$T^1 = T^2 = \ldots = T^\pi \tag{2.21}$$

$$P^1 = P^2 = \ldots = P^\pi \tag{2.22}$$

$$\mu_i^1 = \mu_i^2 = \ldots = \mu_i^\pi \quad i = 1, 2, 3,\ldots \tag{2.23}$$

where μ_i is chemical potential which is equal to the partial molar Gibbs free energy $\bar{g}_i$ and is defined as :

$$\mu_i = \left(\frac{\partial G}{\partial n_i} \right)_{T,P,n_{j \neq i}} \tag{2.24}$$

Chemical potential is a difficult thermodynamic variable to use in the real world because only its relative values can be computed. It is, therefore, desirable to express the chemical potential in terms of a new thermodynamic variable called fugacity, f_i, that might be more easily identified with physical reality (Prausnitz et al. 1999).

It was Lewis-Randall rule that defined a relation between the chemical potential and the fugacity for an isothermal change for any component in any system, solid, liquid, or gas, pure or mixed, ideal or not

$$\mu_i - \mu_i^o = RT \ln \frac{f_i}{f_i^o} \quad (\widehat{f}_i, \text{ for a mixed system}) \tag{2.25}$$

where μ_i^o and f_i^o are arbitrary, but not independent values of chemical potential and fugacity of component *i* for some chosen reference state. Substituting Eq. (2.25) into Eq. (2.23), expression of phase equilibrium at constant and uniform values of the system and pressure is, therefore

$$f_i^1 = f_i^2 = \ldots = f_i^\pi \quad i = 1, 2,..., N \tag{2.26}$$

For all species Eq. (2.26) sometimes referred to as the *isofugacity* condition, has been widely used for phase equilibrium calculations.

The problem in determining equilibrium composition for a reactive system needs a condition and specific information about component in the closed system (Aseyev, 1999). The equilibrium constant for each reaction in a closed system can be derived as

$$K = \prod_i \gamma_i x_i = \exp\left(\frac{-\Delta G}{RT}\right) \tag{2.27}$$

while total Gibbs energy results an equilibrium in general condition, the terms of excess Gibbs energy can be expressed as liquid behavior conveniently.

Excess functions are the excess of thermodynamic properties of solutions compared to those of an ideal solution at the same condition of temperature, pressure, and composition. For an ideal solution all excess functions are zero. A general excess function is defined as

$$e^E = e^{real} - e^{ideal} \tag{2.28}$$

The excess Gibbs free energy as an important excess function is defined by

$$G^E \equiv G_{T,P,x\,\text{actual soln}} - G_{T,P,x\,\text{ideal soln}} \tag{2.29}$$

For phase-equilibrium thermodynamics, the partial molar excess Gibbs free energy is the most useful partial excess property because it is directly related to the activity coefficient. The relation between partial molar excess Gibbs energy and the activity coefficient for a component *i* in solution at constant temperature and pressure is

$$g_i^{ex} = g_i^{real} - g_i^{ideal} = RT\left[\ln f_i^{real} - \ln f_i^{ideal}\right] \tag{2.30}$$

And finally

$$g_i^{ex} = RT \ln \gamma_i \tag{2.31}$$

Equation (2.31) can be rewritten as

$$g^{ex} = RT\sum_{i=1}^{N} x_i \ln \gamma_i \tag{2.32}$$

where g^{ex} is the molar excess Gibbs free energy.

Excess Gibbs energy represents a deviation from ideal behavior in liquid solution. Mathematically, this is the difference between the real and ideal chemical potentials:

$$g_i^{ex} = g_i - g_i^{ideal} \tag{2.33}$$

and partial molar Gibbs energy of species *i*, g_i, is related to the solution fugacity at constant pressure and temperature by

$$g_i = \Gamma_i(T,P) + RT\ln f_i \tag{2.34a}$$

$$g_i^{ideal} = \Gamma_i(T,P) + RT\ln x_i f_i \tag{2.34b}$$

Substituting these general expressions for Gibbs energy into Eq. (2.33) and applying the Lewis/Randall rule, the excess Gibbs energy is directly related to the activity coefficient by

$$g_i^{ex} = RT\ln\frac{f_i}{x_i f_i} = RT\ln\gamma_i \tag{2.35}$$

An open system can exchange matter as well as energy with its surroundings. The number of moles of each component in the system may change. Therefore, the Gibbs free energy, G, an extensive property of the system, can be expressed as a function of temperature, pressure, and the number of moles of each component:

$$G = G(T, P, n_1, n_2, \ldots, n_N) \tag{2.36}$$

where N is the number of components. The total differential of G is then

$$dG = \left(\frac{\partial G}{\partial T}\right)PndT + \left(\frac{\partial G}{\partial P}\right)TndP + \sum_{i=1}\overline{g_i}dn_i \tag{2.37}$$

at constant temperature and pressure Eq. (2.37) reduces to

$$dG = \sum_{i=1} \overline{g_i} dn_i \tag{2.38}$$

where

$$\overline{g}_i = \left(\frac{\partial G}{\partial n_\iota} \right)_{TPn_{j \neq i}} \tag{2.39}$$

The Gibbs free energy is related to the partial molar Gibbs free energy $g_1, g_2, g_3 \ldots, g_n$ by Euler's theorem.

$$G = \sum_{i=1} \overline{g_i} n_i \tag{2.40}$$

Differentiation of Eq. (2.40) gives

$$dG = \sum_{i=1} \overline{g_i} dn_i + \sum_i n_i d\overline{g_i} \tag{2.41}$$

The Gibbs-Duhem equation can be derived from this equation.

The definition of a partial molar property is applicable only to extensive properties (volume V, internal energy U, enthalpy H, entropy S, Helmholtz energy A, and Gibbs free energy G) differentiated at a constant temperature and pressure. For example, the total volume of a mixture is related to the partial molar volumes by a summation.

Most activity coefficient models, such as the ENRTL, rely on minimizing the excess Gibbs free energy of the system. So, the model must find the minimum of the Gibbs energy while satisfying defined equilibrium constant for each reaction. This provides that fluid behavior can be described at an ideal condition, normally infinite dilution in water, as defined by equilibrium constant. Deviation from ideal behavior can be accounted for by activity coefficient model.

2.3 Chemical Potential

As mentioned before, the chemical potential is a difficult thermodynamic variable to use in practical world because one cannot compute its absolute value; but only its change

accompanying any arbitrary change in the independent variables temperature, pressure, and composition. For a pure substance *i*, the chemical potential is related to the temperature and pressure by the differential equation

$$d\mu_i = -s_i dT + v_i dP \tag{2.42}$$

where s_i is the molar entropy

$$s_i = \left(\frac{\partial \mu_i}{\partial T}\right)_P \tag{2.43}$$

and v_i is the molar volume

$$v_i = \left(\frac{\partial \mu_i}{\partial P}\right)_T \tag{2.44}$$

Integrating and solving μ_i at some temperature T and pressure P yields

$$\mu_i(T,P) = \mu_i(T^o, P^o) - \int_{T^o}^{T} s_i \, dT + \int_{P^o}^{P} v_i \, dP \tag{2.45}$$

where superscript *o* refers to some arbitrary reference state.

The chemical potential can be defined in terms of the derivative of the extensive thermodynamic properties (*U*, *H*, *A*, and *G*) with respect to the amount of the component under consideration. Equation (2.45) shows the expression of the chemical potential in terms of Gibbs free energy. The equilibrium condition in terms of the chemical potentials at constant temperature and pressure can be written as

$$dG = \sum_{i}^{N} dn_i = 0 \tag{2.46}$$

Since the chemical potential cannot directly be used in the real world, suitable expressions relating the chemical potential to more convenient quantities are needed.

2.4 Activity and Activity Coefficient

The activity, *a*, of component *i* at some temperature, pressure, and composition is defined as the ratio of the fugacity of component *i* at these conditions to the fugacity of component *i* in

the standard state (Danckwerts, 1951). The activity of a substance gives an indication of how active a substance is relative to its standard state.

$$a_i(T,P,x) \equiv \frac{f_i(T,P,x)}{f_i\,(T,P^\circ,x^\circ)} \qquad (2.47)$$

where subscript o refers to some arbitrary state, arbitrary specified pressure and composition. Substituting Eq. (2.47) into Eq. (2.25) yields a relation between the chemical potential and activity

$$\mu_i - \mu_i^\circ = \mathrm{RT} \ln a_i \qquad (2.48)$$

The activity coefficient γ_i is defined as the ratio of the activity of component *i* to its concentration (usually mole fraction)

$$\gamma_i \equiv \frac{a_i}{x_i} \qquad (2.49)$$

2.5 Electrolyte-Non-Random-Two-Liquid Model, ENRTL

The first significant achievement for activity coefficient expression in dilute electrolyte solutions was made by Debye and Hückel (1923). Modifying that activity coefficient expression was made by several authors such as Guggenheim (1935), Bromley (1973), and Pitzer (1973). An overview of the Debye-Hückel limiting law given here is based on description by Prausnitz et al. (1999).

The activity coefficients of ions in an electrolyte solution strongly depend on concentrations and the number of charges of ions (Harned and Robinson, 1940). This dependence can be expressed in terms of ionic strength of the solution, *I*, defined by

$$I = 1/2 \sum_i^N m_i z_i^2 \quad \mathrm{i} = 1, 2, \ldots, \mathrm{N} \qquad (2.50)$$

where z_i is the charge of ion *i* and m_i its molal concentration.

Due to their velocities, molecules have kinetic energy and they also have potential energy as a result of their positions relative to another. Consider two spherically symmetric molecules

with different charges of magnitudes q_i and q_j separated by a distance r in a vacuum medium, the potential energy Γ shared by these two charged molecules or ions is

$$\Gamma_{ij} = \frac{q_i q_j}{4\pi\varepsilon_\circ r} = \frac{z_i z_j e^2}{4\pi\varepsilon_\circ r} \qquad (2.51)$$

where ε_o is the permittivity of vacuum ($8.85419 \times 10^{-12} C^2\ J^{-1} m^{-1}$), z_i and z_j are ionic valences, and e is the electronic charge (1.60218×10^{-19} C) whereas values of ε_o and e are taken from Archer (1993). For a medium other than vacuum, Eq. (2.51) becomes

$$\Gamma_{ij} = \frac{z_i z_j e^2}{4\pi\varepsilon r} \qquad (2.51a)$$

where ε is the absolute permittivity defined by $\varepsilon = \varepsilon_o, \varepsilon_r$; ε_r is dielectric constant or relative permittivity.

Equation (2.51) shows that the potential energy of interaction varies inversely with the first power of distance. A shielding effect between anion and cation will produce a decrease in their attractions. To account for this effect, the Debye-Hückel theory shows that r^{-1} should be multiplied by a "damping factor"

$$r^{-1} \rightarrow (r^{-1}) \exp(-r\kappa) \qquad (2.52)$$

where κ^{-1} is the *shielding length* or *Debye length* defined by

$$\kappa^{-1} = \left(\frac{\varepsilon RT}{2\rho_s N_A^2 e^2 I} \right)^{1/2} \qquad (2.53)$$

where ρ_s is the solvent density and N_A is the Avogadro's number. From Eq. (2.53), it is clearly seen that the Debye length decreases with rising concentration (ionic strength).

Using well-established concepts from classical electrostatics, Debye and Hückel derived a simple expression for the molar activity coefficient γ_i of an ion with charge z_i in a dilute solution:

$$\ln \gamma_i^{(c)} = - z_i^2 \frac{e^2 N_A}{8\pi\varepsilon RT} \kappa \qquad (2.54)$$

Since there is no significant difference between molarity and molality for dilute aqueous solutions near ambient temperature, for a non volatile solute, it is convenient to use the activity coefficient in the molality scale

$$\ln \gamma_i^{(m)} = - A_\gamma z_i^2 I^{1/2} \qquad (2.54a)$$

where the constant of activity coefficient, A_γ, is given by

$$A_\gamma = \left(\frac{e^2}{\varepsilon RT} \right)^{3/2} \frac{N_A^2}{8\pi} (2\rho_s)^{1/2} \qquad (2.55)$$

Equations (2.54) and (2.54a) give the activity coefficient of ions, not only electrolytes in an electrically-neutral solution. In the experiment, the mean ionic activity coefficient $\gamma_\pm^{(m)}$ is, however, the quantity usually measured. For a 1-1 electrolyte solution, it is defined by

$$\gamma_\pm^{(m)} = -A_\gamma \, |z_+ z_-| I^{1/2} \qquad (2.56)$$

where $|z_+ z_-|$ is the absolute value of the product of the charges. Equation (2.56) is called as the *Debye-Hückel limiting law* which is useful for interpreting the properties of electrolyte solutions.

The Debye-Hückel equation is applicable only to very dilute solutions (typically, for ionic strength up to 0.01 mol/kg). For concentrated electrolyte solutions, several semi-empirical corrections to Debye-Hückel limiting law have been proposed such as

$$\ln \gamma_\pm = - \frac{A_\gamma |z_+ z_-| I^{1/2}}{1 + I^{1/2}} + bI \qquad (2.57)$$

where b is an adjustable parameter. This extended Debye-Hückel equation is only valid up to an ionic strength of ≈ 1 mol/kg which is still much lower than that of many practical industrial applications. When ion concentrations are low, the average distance between ions is large; therefore, only long-range electrostatic forces are important. As ion concentrations rise, ions begin to interact also with hard-core repulsive forces and with short-range (van der Waals) attraction forces. Based on this, later models try to consider the short-range interactions by combining binary and sometimes ternary interaction parameters in their equations.

The mean ionic activity coefficient correlation for an electrolyte solution has been proposed by Guggenheim (1935) based on the combination of an extended Debye-Hückel equation, to account for long-range ion interactions, with a second order virial expansion term, to account for various short-range forces between ions of opposite charge. The Debye-Hückel equation then can be expressed in molality scale as written below:

$$\ln \gamma_{\pm} = -\frac{A_{\gamma}\left|z_{+}z_{-}\right|I^{1/2}}{1+I^{1/2}} + \frac{2v_i}{v_{-}+v_{+}}\sum \beta_{+}^{m} + \frac{2v_i}{v_{-}+v_{+}}\sum \beta_{-}^{m} \qquad (2.58)$$

where v_+ and v_- are number of cations and anions of the electrolyte and β_+ is the interaction coefficient in cation and β_- is interaction coefficient in anion at a given temperature with *m* being scale of molality.

Bromley (1973) also proposed a semi-empirical equation for representing the mean activity coefficient of a single electrolyte or mixed electrolytes in water. The mean ionic activity coefficient correlation for a single salt solution is defined by

$$\ln \gamma_{\pm} = -\frac{A_{\gamma}|z_{+}z_{-}|I^{1/2}}{1+I^{1/2}} + \frac{(0.06+0.06\beta)I|z_{+}z_{-}|}{\left(1+\frac{1.5I}{|z_{+}z_{-}|}\right)^{2}} + \beta I \qquad (2.59)$$

β is taken as a constant, approximated as the sum of individual ion β values. However, the constant is only applicable to ≈ 0.1 molal (Bromley, 1973).

Pitzer (1973) presented an excess Gibbs energy model based on a reformulation and extension of Guggenheim's equation in which the ion-ion short range interactions are important and are dependent on the ionic strength. The excess Gibbs energy for an electrolyte solution containing w_s kilograms of solvent, with molalities of solute species $m_i, m_j, \ldots$ is given by

$$\frac{g^{ex*}}{RT}_{w_s} = f(I) + \sum_i \sum_j m_i m_j \Lambda_{ij} + \sum_i \sum_j \sum_k m_i m_j m_k \Lambda_{ijk} + ... \qquad (2.60)$$

where the function *f(I)*, representing long-range electrostatic forces and including the Debye-Hückel limiting law, depends on ionic strength *I*, temperature, and Λ_{ijk} terms account for three-body ion interactions which are important only at high salt concentration.

Consider the dissociation of an electrically neutral electrolyte $M_{v+}X_{v-}$ in a high-dielectric-constant medium like water

$$M_{v+}X_{v-} \leftrightarrow v_+M^{z+} + v_-X^{z-} \tag{2.61}$$

For this solution containing n_s moles of solvent an n_{MX} moles of completely dissociated electrolyte, the mean ionic activity coefficient of the model of Pitzer is then expressed as

$$\ln \gamma_{\pm}^{(m)} = \frac{1}{(v_+ + v_-)RT}\left(\frac{\partial G^{E^*}}{\partial n_{Mx}}\right)_{P,T,n_s} = |z_+ z_-| f^{\nu} + m\frac{2v_+v_-}{v_+ + v_-}\beta_{Mx}^{\gamma} + x^2\frac{2(v_+v_-)^{3/2}}{v_+ + v_-} \tag{2.62}$$

where f^{γ} and β_{MX}^{γ} are ionic strength dependence and C_{MX}^{γ} depends on triple-ion interactions which is important at high concentration, usually higher than 2 mol/kg (Prausnitz et al. 1999).

The ion-interaction model of Pitzer has achieved wide acceptance and has been applied successfully in such industrial processes such as solubilities of atmospheric gases in seawater and equilibrium of multi component brines with solid phases (Prausnitz et al. 1999).

Deshmukh and Mather (1981) applied the Guggenheim extension of the Debye-Hückel (1923) theory to acid gas-alkanolamine-water solution. The model became very popular among chemical engineers. The expression for coefficient activity used in their work can be written as

$$\ln \gamma_i = \frac{-2.303A_{\gamma}z_i^2 I^{1/2}}{1+\beta a I^{1/2}} + 2\sum_{j\neq w}\beta_{ij}m_{ij} \quad w = \text{water} \tag{2.63}$$

To find rigorous thermodynamic model can be done by employing many models however for vapor-liquid equilibrium which reaction involved, Electrolyte-Non-Random-Two-Liquid (ENRTL) theory may give better approach. This model was initially used by Austgen (1989) for MEA and DEA system in solution with MDEA. Then the model also had been employed by Posey (1996) for MEA and DEA solutions and Bishnoi and Rochelle (2002) for PZ/MDEA blends. For the work of this thesis the model will be used for potassium carbonate solution.

Description of the theory about ENRTL model and gas phase calculations will be explained in the following sections briefly. Furthermore, the complete description of the model theory, construction, and solution method can be found in Chen et al. (1982, 1986), Mock et al. (1986), Austgen (1989), and Glasscock (1990).

Chen et al. (1982) initially developed the ENRTL model as an extension to the existing theory for dilute electrolyte solutions. The ENRTL model mean to predict solution behavior of concentrated electrolytes better than the applicable range of Pitzer-Debye-Hückel model or other theoretical activity coefficient models. Since its inception, the model has been applied in widespread industrial use particularly for simulation of gas treating processes (Chen and Mathias, 2002).

The ENRTL model describes both dilute and concentrated electrolyte solutions activities. The dilute solutions are assumed that molecules are separately far and the excess Gibbs energy is dominated by long range (LR) forces. There are two others contribution, Pitzer-Debye-Hückel (PDH) and Born. The two contributions to long range forces, PDH and Born will be discussed later. In concentrated solutions, the molecules will have closely interaction with one another and in this condition the ENRTL model gives assume that short range (SR) interactions contributes dominantly. The overall contribution to excess Gibbs free energy can be expressed below:

$$\frac{g_i^{ex*}}{RT} = \frac{g_{LR,i}^{ex*}}{RT} + \frac{g_{SR,i}^{ex*}}{RT} = \left(\frac{g_{PDH,i}^{ex*}}{RT} + \frac{g_{Born,i}^{ex*}}{RT} \right) + \frac{g_{NRTL,i}^{ex*}}{RT} \tag{2.64}$$

or from Eq. (2.35) above can be represented as

$$\ln \gamma_i = \left(\ln \gamma_{PDH,i} + \ln \gamma_{Born,i} \right) + \ln \gamma_{NRTL,i} \tag{2.65}$$

2.5.1 Long Range Forces

Pitzer-Debye-Hückel Model

In dilute solutions (< 1 M), to describe excess Gibbs free energy in theoretical relationship with ionic interactions is presented below

$$g_{PDH}^{ex*} = RT \left(\sum_i x_i \right) \left(\frac{1000}{MW} \right)^{0.5} \left(\frac{4 I_x A_\phi}{\rho} \right) \ln\left(1 + \rho I_x^{0.5}\right) \tag{2.66}$$

the asterisk in equation above shows as the asymmetric excess Gibbs free energy, x is the mole fraction, MW is molecular weight of the solvent and ρ is the density of solution. I_x is the ionic strength for mole fraction and charge, z

$$I_x = \frac{1}{2}\sum_i z_i^2 x_i \tag{2.67}$$

Using N_o, Avogadro's number, ρ_s, solvent density; e, electron charge; D_s, dielectric constant of the solvent; and k, Boltzmann constant to find The Debye-Hückel parameter, A_{ϕ}.

$$A_\phi = \frac{1}{3}\left(\frac{2\rho_s N_o}{1000}\right)^{0.5}\left(\frac{e^2}{kTD_s}\right) \tag{2.68}$$

Calculation for solvent dielectric constant can be done by equation below:

$$D_s = \sum_i x_i D_i \tag{2.69}$$

x_i = mass fraction.

D_s = the dielectric constant of species *i*.

The dielectric constants for water and piperazine are shown in Table 2.1

Table 2.1 Dielectric constant of Molecular Species in the ENRTL Model.

$D_i = A + B\left(\frac{1}{T} + \frac{1}{273.15}\right)$ T in Kelvin			
Species	**A**	**B**	**Source**
Water	88.365	33030	Helgeson (1970), Bishnoi and Rochelle (2000)
Piperazine (assumed)	4.719	1530	Handbook of Chemistry and Physics (2000)

Born Equation

In mixed solvents, the reference state for ions is not completely found because of the changing dielectric constant. The Born equation then was applied in the long range contributions to Gibbs energy to keep a reference state of infinite dilution of water for the ions. The correction of the form is written below:

$$g_{Born}^{ex} = RT\left(\frac{e^2}{2kT}\right)\left(\sum_i \frac{x_i z_i^2}{r_i}\right)\left(\frac{1}{D_m} - \frac{1}{D_w}\right) \tag{2.70}$$

As shown in the equation above, D_m and D_w represents the dielectric constants of the mixed solvent and water, respectively (Harned and Owen, 1958). This correction is to fit the difference in Gibbs energies between ions in a mixed solvent and water.

2.5.2 Short Range Forces (Non Random Two Liquid Model)

As the solutions become more concentrated, the requirement to describe interactions between neutral and ionic species and neutral and neutral species is important. These interactions will be assumed as local or short range forces.

Wilson (1964) initially gave mathematical derivation of an equation for excess free energy in the mixed non-electrolytes. The reference for derivation is a distribution of molecules i and j, around a central molecule, i which is expressed below:

$$\frac{x_{ji}}{x_{ii}} = \frac{x_j e^{\frac{-g_{ji}}{RT}}}{x_i e^{\frac{-g_{ii}}{RT}}} \tag{2.71}$$

Renon and Prausnitz (1968) then embedded the assumptions of Wilson into the non-random two liquid (NRTL) model, resulting in a modification of the molecular distribution to the term "non-randomness" of mixing.

$$\frac{x_{ji}}{x_{ii}} = \frac{x_j e^{-\frac{g_{ji}}{RT}\alpha_{ij}}}{x_i e^{-\frac{g_{ii}}{RT}\alpha_{ij}}} \tag{2.72}$$

where α is an adjustable parameter. The values for α are suggested to be ranging between 0.1 and 0.4 which are dependence to the molecules and solvent in the system. The addition of the non-randomness parameter, α, provides wide range application of the model to a better variety of solutions.

An expression for the Gibbs free energy of mixing is taken by both of Wilson and NRTL models in formulation:

$$\frac{g^M}{RT} = \sum_i x_i \ln \xi_i \tag{2.73}$$

where ξ is the volume fraction of *i* around a central molecule. Derivation of volume fraction is extracted from the molecular distributions given above and can be written as

$$\xi_i = \frac{x_i v_i \exp\left(\frac{g_{ij}}{RT}\right)}{\sum_j x_j v_j \exp\left(\frac{g_{ij}}{RT}\right)} \tag{2.74}$$

where v represents the molar volume. The energy of mixing is then contributed to the excess Gibbs energy by

$$\frac{g^{ex}}{RT} = \frac{g^M}{RT} - \sum_i x_i \ln x_i \tag{2.75}$$

Chen et al. (1982, 1986) added extension to this equation for multi component solutions of neutral and ionic species. The recent version of this model involved three distinct cells, or group of interacting ions and molecules as drawn in Fig. 2.2. They assumed two approachments for the physical description of interacting species.

1. Two cells include a central cation, c, or a central anion, a. They are assumed like ion repulsion so that the central ion is surrounded by molecules and oppositely charged ions.
2. One cell consists of a centrally located molecule, m, with local electro neutrality, referring that a time-average charge around the central molecule equals zero.

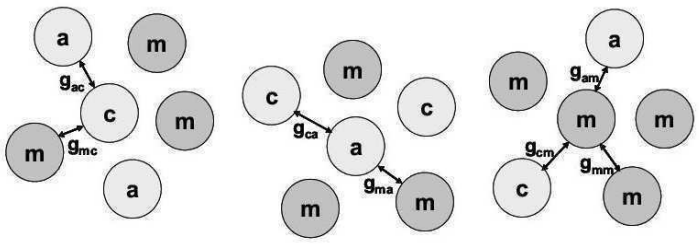

Figure 2.2 Distributions of molecules as cells in the ENRTL theory

Specific references for two interacting species are described in multiple interactions within cells. In other words, modeling the Gibbs energy contribution as a function of binary interactions can be defined as

$$\tau_{ji,ki} = \frac{g_{ji} - g_{ii}}{RT} \tag{2.76}$$

An overall model, therefore, is constructed to estimate the sum of the specific interactions in the species within an average solution composition.

The excess Gibbs energy prediction from the NRTL theory is written below:

$$\frac{g^{ex}_{NRTL}}{RT} = \sum_m \left(X_m \frac{\sum_j X_j G_{jm} \tau_{jm}}{\sum_k X_k G_{km}} \right) + \sum_c X_c \left(\sum_{a'} \left(\frac{X_a \sum_j G_{jc,a'c} \tau_{jc,a'c}}{\sum_{a''} X_{a''} \sum_k X_k G_{kc,a'c}} \right) \right)$$

$$+ \sum_a X_a \left(\sum_{c'} \left(\frac{X_{c'} \sum_j G_{ja,c'a} \tau_{ja,c'a}}{\sum_{c''} X_{c''} \sum_k X_k G_{ka,c'a}} \right) \right) \tag{2.77}$$

where

$$G_{cm} = \frac{\sum_a X_a G_{ca,m}}{\sum_{a'} X_{a'}}, \; G_{am} = \frac{\sum_c X_c G_{ca,m}}{\sum_{c'} X_{c'}} \tag{2.78}$$

$$G_{jc,a'c} = \exp\left(-\alpha_{jc,a'c}\tau_{jc,a'c}\right), \; G_{ja,c'a} = \exp\left(-\alpha_{ja,c'a}\tau_{ja,c'a}\right) \tag{2.79}$$

and

$$G_{im} = \exp\left(\alpha_{im}\tau_{im}\right), \quad G_{ca,m} = \left(-\alpha_{ca,m}\tau_{ca,m}\right) \tag{2.80}$$

$$\alpha_{cm} = \frac{\sum_a X_a \alpha_{ca,m}}{\sum_{a'} X_{a'}}, \; \alpha_{am} = \frac{\sum_c X_c \alpha_{ca,m}}{\sum_{c'} X_{c'}} \tag{2.81}$$

also, $\tau_{ma,ca} = \tau_{am} - \tau_{ca,m} + \tau_{m,ca}$, $\tau_{mc,ac} = \tau_{cm} - \tau_{ca,m} + \tau_{m,ca}$, $X_j = x_j C_j$ ($C_j = Z_j$ for ions and 1 for molecules), α is non-randomness parameter, and τ is the binary interaction parameter.

The reference state of NRTL contribution can be referred to the unsymmetric convention associated with the correction of infinite dilution activity coefficients:

$$\frac{g^{ex*}_{NRTL}}{RT} = \frac{g^{ex*}_{NRTL}}{RT} - \left(\sum_{m \neq w} X_m \ln \gamma^{\infty}_m + \sum_c X_c \ln \gamma^{\infty}_c + \sum_a X_a \ln \gamma^{\infty}_a \right) \tag{2.82}$$

where

$$\ln \gamma^{\infty}_m = \tau_{wm} + G_{mw}\tau_{mw} \tag{2.83}$$

$$\ln \gamma^{\infty}_c = Z_c \left(G_{cw}\tau_{cw} + \frac{\sum_{a'} X_{a'} \tau_{wc,a'c}}{\sum_{a''} X_{a''}} \right) \tag{2.84}$$

$$\ln \gamma^{\infty}_a = Z_a \left(G_{aw}\tau_{aw} + \frac{\sum_{c'} X_{c'} \tau_{wa,c'a}}{\sum_{c''} X_{c''}} \right) \tag{2.85}$$

and the subscript *w* represents water.

2.6 Thermodynamic Model Default Settings

For some mixture component such as K+/PZ model, non-randomness parameters for molecule-molecule pairs and water-ion pairs were set to 0.2 based on the recommendation of Renon and Prausnitz (1968). For amine ion pairs, values were set to 0.1. Molecule-molecule interaction parameter τ is given by

$$\tau = A + \frac{B}{T} \tag{2.86}$$

The default value of A is 0.0 and the default temperature dependence, B, is 0.0. The interaction parameter for molecule-ion pair is given by

$$\tau = A + B\left(\frac{1}{T} - \frac{1}{353.15} \right) \tag{2.87}$$

with default values for A and B of 1.5 and -8.0 respectively in equation (2.87). If water is applied for the molecule, the values are 8.0 and -4.0. The default temperature dependence, B, is 0.0. Ion pair interactions are normally insignificant and not included in this model.

2.7 Reference State

Reference state for water and potassium carbonate is in the form of the symmetric convention. This means the activity coefficient for water is easily converted as

$$\gamma_w \rightarrow 1 \quad \text{as} \quad x_w \rightarrow 1 \tag{2.88}$$

However CO_2, ions, and H+COO- are the nonsymmetric convention, the activity coefficients should be referenced to pure water so that

$$\gamma_i^* \rightarrow 1 \quad \text{as} \quad x_i \rightarrow 0 \tag{2.89}$$

The two conventions are related by

$$\frac{\gamma_i}{\gamma_i^*} = \lim_{x_{i\rightarrow 0}} \gamma_i = \gamma_i^{\infty} \tag{2.90}$$

where γ_i^{∞} represents the symmetrically normalized activity coefficient of solute *i*, or the value of γ_i as the solution is similar to pure water as reference state.

The structure of model treats K_2CO_3 as solvent, resulting in two definitions of equilibrium constants that contain K_2CO_3. Constants are normally reported in literature as referenced to infinite dilution water and can be represented as

$$K_{Am}^* = \frac{x_{Am} x_{H30+}}{x_{AmH+} x_{H_2O}} \cdot \frac{\gamma_{Am}^* \gamma_{H3O+}^*}{\gamma_{AmH+}^* \gamma_{H2O}^*} \tag{2.91}$$

The constants utilized in the model are constructed as normal model

$$K_{Am} = \frac{x_{Am} x_{H30+}}{x_{AmH+} x_{H_2O}} \cdot \frac{\gamma_{Am}^* \gamma_{H3O+}^*}{\gamma_{AmH+}^* \gamma_{H2O}^*} \tag{2.92}$$

The constants are therefore connected to

$$K_{Am} = K^*_{Am} \frac{\gamma_{Am}}{\gamma^*_{Am}} = K^*_{Am} \gamma^{\infty}_{Am} \quad (2.93)$$

Correction of equilibrium constants for the infinite dilution activity coefficient of K_2CO_3 is required as the unsymmetric convention. Noting that K_2CO_3 is considered as liquid; the requirement of this assumption is that the vapor pressure of K_2CO_3 is represented by liquid K_2CO_3 (Apelblat, 1982). The consequence of this assumption is that equilibrium constants, enthalpies, and other properties relating to K_2CO_3 behavior are referenced as liquid.

2.8 Non-Stoichiometric Method

Non stoichiometric could be applied to solve for equilibrium composition. For instance, Cullinane (2002) showed that K^+/COO^- mixtures from total system properties (total K^+ and COO^-, total CO_2, and temperature) could define the activity coefficients and equilibrium constants through a rigorous model, such as ENRTL model. The Gibbs energy of the solution then can be calculated. For a defined system, the algorithm is used to minimise the Gibbs free energy within the constraints of material balances. The Gibbs energy is able to correlate to the chemical potential and the activity coefficients.

Cullinane (2002) in his investigation particularly when K^+/COO^- mixtures system is applied, there are several unknown species to be considered. Potassium ion, though constant, is considered as an unknown species contributing to increase model flexibility for future applications. Hydronium ion (H_3O^+) can be neglected because its concentration is assumed to be very small. There were five elements identified for the material balances where K^+, COO^-, C, H, and O. COO^- could be as considered an element because it is the core of the molecule and the concentration is constant. The material balances are then

$$n_{K^+} + n_{KH^+} = n_{K^+,\text{tot}} \quad (2.94a)$$

$$n_{COO} + n_{KCOO^-} + n_{KCOO^-H^+} + n_{K(COO)_2^-} = n_{COO,\text{tot}} \quad (2.94b)$$

$$n_{CO_2} + n^{2-}_{CO_3} + n_{HCO_3^-} + n_{KCOO^-} + n_{KCOO^-H^+} + 2n_{K(COO)_2^-} = n_{C,\text{tot}} \quad (2.94c)$$

$$2n_{H2O} + n_{OH^-} + n_{HCO3^-} + 3n_{KH^+} = n_{H,\text{tot}} \quad (2.94d)$$

$$n_{H_2O} + n_{OH^-} + 2n_{CO_2} + 3n_{CO_3^{2-}} + 3n_{HCO_3^-} + 2n_{KCOO^-} + 2n_{KCOO^-H^+} + + 4n_{K(COO)_2^-} = n_{O,\text{tot}} \quad (2.94e)$$

Using Lagrangian multipliers, λ, for each element so that the chemical potential of each species can be expressed as

$$\mu_{CO2} - \lambda_C - 2\lambda_O = 0 \quad (2.95a)$$

$$\mu_{K^+} - \lambda_{K^+} = 0 \quad (2.95b)$$

$$\mu_{H2O} - 2\lambda_H - \lambda_O = 0 \quad (2.95c)$$

$$\mu_{HCO3^-} - \lambda_C - \lambda_H - 3\lambda_O = 0 \quad (2.95d)$$

$$\mu_{CO3^{2-}} - \lambda_C - 3\lambda_O = 0 \quad (2.95e)$$

$$\mu_{OH^-} - \lambda_H - \lambda_O = 0 \quad (2.95f)$$

$$\mu_K - \lambda_K - 2\lambda_H = 0 \quad (2.95g)$$

$$\mu_{KH^+} - \lambda_K - 3\lambda_H = 0 \quad (2.95h)$$

$$\mu_{KCOO^-} - \lambda_K - \lambda_C - \lambda_H - 2\lambda_O = 0 \quad (2.95i)$$

$$\mu_{KCOO^-H^+} - \lambda_K - \lambda_C - 2\lambda_H - 2\lambda_O = 0 \quad (2.95j)$$

$$\mu_{K(COO^-)_2} - \lambda_K - 2\lambda_C - 4\lambda_O = 0 \quad (2.95k)$$

These eleven equations which are dependent upon chemical potential, then should be solved simultaneously. The chemical potentials are minimized and an equilibrium composition is calculated. A complete calculation of non-stoichiometric method and the solution algorithm by Smith and Missen (1988) can be found in Austgen (1989).

CHAPTER 3

METHODOLOGY

A good model is needed in order to obtain solubility of carbon dioxide in potassium carbonate solution. Even though not all the models are right but some of them are useful; an effective model is itself an abstraction of the real world with the ability to capture enough detail to be realistic. Hence, models can be useful and powerful tools; an indispensable aid to research and a corner stone to industrial project applications.

This chapter describes methodology to predict and find solubility of carbon dioxide in potassium carbonate solution with the electrolyte non-random two-liquid model including the constants and equation used in this work. The first section will discuss basic scalar properties, chemical reaction equilibrium constant which is useful to give data for solubility prediction especially for the K_2CO_3-H_2O-CO_2 system. The chemical constants are expressed in terms of activity coefficients. Element and component ionic then was classified to describe total ionic in matrix form, after each mol fraction was obtained activity coefficient was calculated with ENRTL models. Henry's constant for carbon dioxide in the solution was connected to the Henry's constant of carbon dioxide in water through the activity coefficient.

3.1 K_2CO_3-H_2O-CO_2 System

Carbon dioxide can be soluble in potassium carbonate by formation of HCO_3^{-1} ion in the liquid phase. Figure 3.1 illustrates the predictive system for the solubility of carbon dioxide in aqueous solution of potassium carbonate (Cullinane, 2005) with the following reactions taking place in the aqueous phase:

R_1: $H_2O \leftrightarrow H^+ + OH^-$ (3.1)

R_2: $CO_2 + H_2O \leftrightarrow H^+ + HCO_3^-$ (3.2)

R_3: $HCO_3^- \leftrightarrow H^+ + CO_3^{2-}$ (3.3)

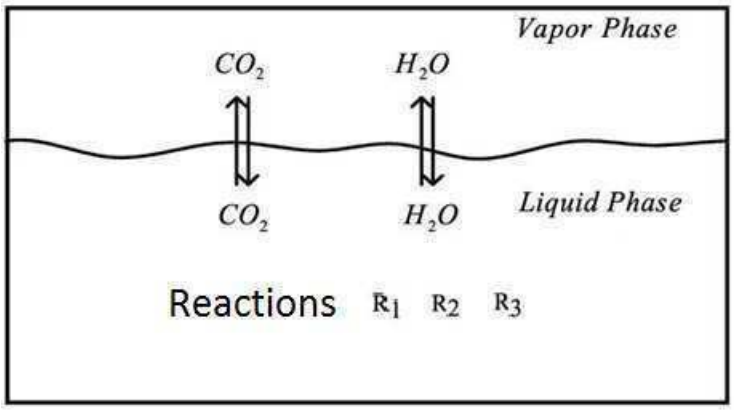

Figure 3.1 Chemical reaction of CO_2-K_2CO_3.

Reaction (3.1) gives the ionization of water to proton (H+) and hydroxide ions (OH^-); Reaction (3.2) shows the hydrolysis and ionization of dissolved CO_2 to H^+ and bicarbonate ions (HCO_3^-); Reaction (3.3) describes the dissociation of HCO_3^- to H^+ and carbonate ions (CO_3^{2-}). The chemical equilibrium constants for all reaction above are expressed in terms of the activity of component *i* as expressed by the following relationship:

$$K_j = \prod_i a_i^{v_{i,j}} \quad (3.4)$$

where: K_j is the chemical equilibrium constant; $v_{i,j}$ is the reaction stoichiometric coefficient of component *i*; and a_i is the activity of component *i*.

In this work we define the chemical equilibrium constants with temperature dependence as:

$$\ln K_i = A + \frac{B}{T} + ClnT + DT \quad (3.5)$$

The previous framework may provide precise thermodynamic model to be internally suitable with respect to the governing thermodynamic definitions. Tables 3.1 and 3.2 present standard state conditions at 25 ºC related to the species in the Reactions (3.1) to (3.3). Standard state conditions are extracted from the published literature by Edwards et al. (1978).

The changes in Gibbs free energy of reaction could be related to chemical potential standart of elements as stated below

$$RT \ln K_i = -\sum_{i=1}^{N} a_i \mu_i^{\circ} \tag{3.6}$$

where μ_i° is chemical potential standard of species

Table 3.1 Standard State Property Values for Reactions of CO_2-K_2CO_3.

Species	Gf° (kCal/mole)	Hf° (kcal/mole)
$H^2O_{(l)}$	-56.6828	-68.2755
$H^+_{(aq)}$	0	0
$OH^-_{(aq)}$	-37.5571	-54.9331
$CO_{2(aq)}$	-92.18974	-98.83443
$CO_3^{2-}{}_{(aq)}$	-128.584	-161.7321
$HCO_3^-{}_{(aq)}$	-140.291	-164.9871

Table 3.2 Chemical Equilibrium Coefficients for H_2O-K_2CO_3-CO_2 System.

Equation	A	B	C	D
3.1	132.8989	-13445.9	-22.4773	0
3.2	231.4654	-12092.1	-36.7816	0
3.3	216.0504	-12431.7	-35.4819	0

The standard property changes of reaction (e.g. Gibbs free energy and enthalpy) are referred as the difference between the standard property change of the products and reactants, accounted by their stoichiometric coefficients

$$\Delta^{\circ} M = \sum_i \nu_i M_i^{\circ} \tag{3.7}$$

For molecular solutes (e.g. CO_2), the standard Gibbs free energy can be expressed as basis to the ideal gas reference state by the following equation:

$$G_{CO_2}^{\circ}(\mathrm{T}) = G_{CO_2}^{ig}(T) + RT ln \frac{H_{CO_2}(T)}{P^{ref}} \tag{3.8}$$

where $G_{CO_2}^{\circ}$ is the ideal gas Gibbs free energy, J/mol, H_{CO_2} is the Henry's constant for CO_2 in H_2O atm (Chen et al. 1979), and P^{ref} is reference pressure of 1 atm.

For a given temperature, a rigorous development initiated with the following equation:

$$\Delta G_m^\circ = \Delta H_m^\circ - T\Delta S_m^\circ \tag{3.9}$$

Equation (3.9) is source of definition about the molar Gibbs free energy applied to each component in a chemical reaction evaluated at standard state. Substituting Eqs. (3.7) to (3.9) yields

$$\sum_i v_i G_{m,i}^\circ = \sum_i v_i H_{m,i}^\circ + T\sum_i v_i S_{m,i}^\circ \tag{3.10}$$

where the standard molar heat of reaction and standard molar entropy change of reaction are dependance to temperature by the following expressions

$$\Delta H_m^\circ = \Delta H_{0,m}^\circ + R\int_{T_0}^{T} \frac{\Delta C_{p,m}^\circ}{R} dT \tag{3.11}$$

$$\Delta S_m^\circ = \Delta S_{m,0}^\circ + R\int_{T_0}^{T} \frac{\Delta C_{p,m}^\circ}{R} \frac{dT}{T} \tag{3.12}$$

Equation (3.9) together with eqs. (3.11) and (3.12) are combined to form

$$\Delta G_m^\circ = \Delta H_{0.m}^\circ + R\int_{T_0}^{T} \frac{\Delta C_{p,m}^\circ}{R} dT - T\Delta S_{0,m}^\circ - RT\int_{T_0}^{T} \frac{\Delta C_{p,m}^\circ}{R} \frac{dT}{T} \tag{3.13}$$

However

$$\Delta S_{0,m}^\circ = \frac{\Delta H_{0,m}^\circ - \Delta G_{0,m}^\circ}{T_0} \tag{3.14}$$

Hence

$$\Delta G_m^\circ = \Delta H_{0,m}^\circ - \frac{T}{T_0}\left(\Delta H_{0,m}^\circ - \Delta G_{0,m}^\circ\right) + R\int_{T_0}^{T} \frac{\Delta C_{p,m}^\circ}{R} dT - RT\int_{T_0}^{T} \frac{\Delta C_{p,m}^\circ}{R} \frac{dT}{T} \tag{3.15}$$

Finally, all the equations divided by RT yields

$$-lnK_i = \frac{\Delta G_m^\circ}{RT} = \frac{\Delta G_{0,m}^\circ - \Delta H_{0,m}^\circ}{RT_0} + \frac{\Delta H_{0,m}^\circ}{RT} + \frac{1}{T}\int_{T_0}^{T} \frac{\Delta C_{p,m}^\circ}{R} dT - \int_{T_0}^{T} \frac{\Delta C_{p,m}^\circ}{R} \frac{dT}{T} \tag{3.16}$$

Chemical equilibrium constants calculated following the above convention are on molality basis. In addition, chemical equilibrium noted in literature is normally referenced to infinite

dilution in water (molality based), assuming potassium carbonate and bicarbonate as solutes. The properties such as solutes and ionic activity coefficients are preferred to the asymmetric reference state convention which states that as the activity coefficient reaches one, the mole fraction of the species approaches zero in pure water.

Based on the asymmetric reference state convention, the chemical equilibrium constant of some dilute solution such as monoethanolamine requires an additional conversion (Danckwerts and Sharma, 1966). For the symmetric reference state convention, since all subsequent dilute solution related to ionic equilibrium constants, are determined on the asymmetric reference state convention referenced to infinite dilution in the solution. These two reference state conventions can be expressed as the following form:

$$\frac{\gamma_{Amine}}{\gamma^*_{Amine}} = \lim_{x_{Amine}\to 0} \gamma_{Amine} = \gamma^{\infty}_{Amine} \tag{3.17}$$

where γ_{Amine} is the symmetric activity coefficient for the solution of amnine and γ^*_{Amine} is the asymmetric activity coefficient it approaches its pure amine solute reference state.

3.1.1 Element Balances

Once the chemical equilibrium constants are determined, the element and component balances need to be derived as well. Equation for element and component balances can be found in Cullinane (2005). The element balances to be used are:

$$2n_{H_2O} + n_{HCO_3^-} + n_{OH^-} + 3n_{H_3O^+} = n_{H,Tot} \tag{3.18a}$$

$$n_{CO_2} + n_{CO_3^{2-}} + n_{HCO_3^-} = n_{C,Tot} \tag{3.18b}$$

$$n_{H_2O} + 2n_{CO_2} + 3n_{CO_3^{2-}} + 3n_{HCO_3^-} + n_{OH^-} + n_{H_3O^+} = n_{O,Tot} \tag{3.18c}$$

and the equation for electro neutrality balance:

$$2n_{CO_3^{2-}} - n_{HCO_3^-} - n_{OH^-} - n_{H_3O^+} + n_{K^+} = 0 \tag{3.19}$$

Element balances is defined into a matrices form to find chemical potential standard of element by using Gauss Elimination method. Langrange multiplier was introduced for each element so the chemical potentials could be expressed by:

$$\mu_{H_2O} + 2\lambda_H + \lambda_O = 0 \quad (3.20a)$$

$$\mu_{CO_2} + \lambda_C + 2\lambda_O = 0 \quad (3.20b)$$

$$\mu_{CO_3^{2-}} + \lambda_C + 3\lambda_O = 0 \quad (3.20c)$$

$$\mu_{HCO_3^-} + \lambda_H + \lambda_C + 3\lambda_O = 0 \quad (3.20d)$$

$$\mu_{H_3O^+} + 3\lambda_H + \lambda_O = 0 \quad (3.20e)$$

$$\mu_{OH^-} + \lambda_H + \lambda_O = 0 \quad (3.20f)$$

$$\mu_{K^+} + \lambda_{K^+} = 0 \quad (3.20g)$$

Total equations above are seven depending on values of chemical potential which are going to be solved simultaneously. Chemical potential is then reduced and the equilibrium composition could be found (Glasscock and Rochelle, 1989).

3.1.2 Lagrange Multiplier

Lagrange multiplier was used to find chemical potential of element by following equation

$$L(n,\lambda) = \sum_{i=1}^{N} n_i \mu_i + \sum_{j=1}^{M} \lambda_j \left(b_j + \sum_{i=1}^{N} a_{ji} n_i \right) \quad (3.21)$$

where a is element and b is total element employed in the reactions

As mentioned before in non stoichiometric solution, we need to minimize chemical potential in order to find equilibrium composition. Condition of minimum chemical potential can be written in equation below

$$\left(\frac{\partial L}{\partial n_i}\right)_{i\neq j,\lambda} = \mu_i - \sum_{i=1}^{N} a_{ij}\lambda_i = 0 \tag{3.22}$$

and

$$\left(\frac{\partial L}{\partial \lambda_i}\right)_{i\neq j,n} = b_j - \sum_{i=1}^{N} a_{ji} n_i = 0 \tag{3.23}$$

If the chemical potential is a dimensionless property, then Eq. (3.22) can be rewritten as

$$\frac{\mu_i}{RT} - \sum_{i=1}^{N} a_{ij}\frac{\lambda_i}{RT} = 0 \tag{3.24}$$

For non ideal solution chemical potential is formulated

$$\mu_i = \mu_i^{\circ} + RT\ln x_i + RT\ln\gamma_i \tag{3.25}$$

Substituting Eq. (3.24) and into Eq. (3.25) resulted

$$\frac{\mu_i}{RT} = \frac{\mu_i^{\circ}}{RT} + \ln x_i + \ln\gamma_i + \sum_{i=1}^{N} a_{ij}\frac{\lambda_i}{RT} \tag{3.26}$$

Equation (3.27) above is the reference calculation to predict activity coefficient in ENRTL model obtaining chemical composition in equilibrium condition.

3.1.3 Henry's Constant

For supercritical gases, Henry's constants plays important role particularly in determining the vapor-liquid equilibrium. Applying Henry's constant model is used when Henry's law needs utilization of molecular solutes in enthalpy and aqueous chemistry algorithm.

In this work, reference state for the activity coefficient of molecular solutes (i.e. CO_2) can be expressed in a volume weighted mixing rule to describe the Henry's constant of CO_2 in mixed solvent as shown below

$$\ln\left(\frac{H_i}{\gamma_i^{\infty}}\right) = \sum_a w_a \ln\left(\frac{H_{i,a}}{\gamma_{i,a}^{\infty}}\right) \tag{3.27}$$

This convention normalizes the reference state of CO_2 to infinite dilution in solution, but for loaded potassium carbonate solutions the reference state for the activity coefficient of CO_2 at infinite dilution is not zero; therefore to account for this, asymmetric activity coefficient can be defined as

$$\gamma_i^* = \frac{\gamma_i}{\gamma_i^{\infty}} \tag{3.28}$$

We could calculate γ_i^{∞} at any loading by setting the CO_2 concentration to zero while allowing all of the other ionic species to remain at the loaded concentration values. This results in a floating reference state for CO_2 and for other CO_2-related species as a function of loading.

In this work, the option to describe the reference state of molecular solutes in infinite dilution in water to be consistent with the ionic component reference state is chosen. This distinction implies that only a correlation expressing the Henry's constant for CO_2 in water is required within the ENRTL model. The Henry's constant for CO_2 in water can be described by the following expression

$$\ln H_i\left(T, P^o_{H_2O}\right) = C_1 + \frac{C_2}{T} + C_3 \ln T + C_4 T + \frac{C_5}{T^2} \tag{3.29}$$

where H_i is the Henry's constant for CO_2 in H_2O at the system temperature and saturation pressure of water, $P^{\circ}_{H_2O}$.

Table 3.3 gives the coefficients used for finding the Henry's constant for CO_2 in H_2O given by Chen et al. (1979) based on equation (3.29).

Table 3.3 Henry's Constant Coefficients of CO_2 in H_2O (Pa/mole fraction).

$\ln H_i = \frac{C_2}{T} + C_3 \ln T + C_4 T + \frac{C_5}{T^2}$				
C_1	C_2	C_3	C_4	C_5
170.7126	-8477.711	-21.95743	0.005781	0

Solubility of CO_2 could be described in water by using the Chen et al. (1979) correlation for Henry's constant for CO_2 in H_2O who developed their correlation based on the experimental work of Ellis and Golding (1963).

3.2 Activity Coefficient Model

For ENRTL framework model the molar Gibbs free energy is given in the following form:

$$G_m^* = x_w \mu_w^* + \sum_k \mu_k \mu_k^* + \sum_j x_j \ln x_j + G_m^{*E} \tag{3.30}$$

where the excess Gibbs free energy associated with ENRTL is given in the following form:

$$\frac{G_m^{*E}}{RT} = \frac{G_m^{*E,PDH}}{RT} + \frac{G_m^{*E,Born}}{RT} + \frac{G_m^{*E,lc}}{RT} \tag{3.31}$$

where PDH is Pitzer-Debye-Hückel contribution for long range ion-ion interactions, Born is Born correction for change in mixed solvent reference state, lc is local contribution for short range interactions.

Pitzer-Debye-Hückel (PDH) model is part of ionic interaction description in long range forces for dilute solution. The equation used for predicting the activity coefficient in ENRTL model is correlated to Gibss free energy in PDH model as presented below

$$\ln \gamma_i^{PDH} = \frac{g_{i,PDH}^{ex}}{RT} = \left(\sum_i x_i \right) \left(\frac{1000}{MW} \right)^{0.5} \left(\frac{4 I_x A_\phi}{\rho} \right) \ln\left(1 + \rho I_x^{0.5}\right) \tag{3.32}$$

The parameters interaction used in PDH model is A_ϕ, Debye-Hückel parameter and I_x, ionic strength. Both of those parameters put dielectric constants of solvent to assume ionic stability during molecular activities in reaction.

Since PDH model only gives ion interaction in dilute solution, it doesn't explain how electrolyte solutions interact with its solvent dilution. To describe electrolyte solutions interaction in mixed solvent Born equation is employed. Born equation is correction in long

range forces together with PDH model to fit better assumption about ionic interaction. Born equation is almost similar to the PDH model which is used dielectric constant and ionic strength but it also applies compound surface parameters to extend description of mass transfer between gas bubble and aqueous solution and extends the dielectric constant for water as solvent solution. Compound surface parameters are required in Born equation since not all of compound surface area hold the absorption process. Activity coefficients of species in Born equation can be rewritten from eq. (2.70) as

$$\ln \gamma_i^{Born} = \frac{g_{i,Born}^{ex}}{RT} = \left(\frac{e^2}{2kT} \right) \left(\sum_i \frac{x_i z_i^2}{r_i} \right) \left(\frac{1}{D_m} - \frac{1}{D_w} \right) \tag{3.33}$$

where r_i is the compound surface parameters for ionic species and D_m is dielectric constants of water taken from Bishnoi and Rochele (2000).

When solution is more diluted, interaction between neutral and ionic species needs to be paid attention. In order to define interaction in diluted solution, the short range forces or local contribution is required. The local contribution equation used in ENRTL model is formulated in eq. (2.37), yet it is easier to formulate the local contribution which is related to surface (r) and volume parameters (Q) for any compounds in the absorption process as written below

$$\xi_i = \frac{x_i r_i Q_i}{\sum_{i=1}^{N} x_i r_i Q_i} \tag{3.34}$$

Volume parameters becomes important in local contribution since concentrated solutions tends to raise volume fraction of central molecule as expressed by Wilson (1964).

The electrolyte non random two liquid model is an appropriate model for estimating activity coefficient particularly when ion interactions are present in electrolyte solutions. There are two assumptions to describe the electrolyte NRTL model

- The ion-ion repulsion: forces around ion charge is considered extremely large so that local composition of cations upon cations is zero (as for anions also) and repulsive forces between ions of the similar sign is quite strong to gather neighboring species.

- The local electro neutrality: the net local ionic charge becomes zero since the distribution of cations and anions around central molecular species tends to possessing equal strong forces.

The model of excess Gibbs free energy contributing to long range ion-ion interactions and the other related to the local interactions present at around any central species is representation of ENRTL model. To complete the model, the unsymmetric Pitzer-Debye-Hückel (PDH) and Born equation is applied to represent the long-range ion-ion interactions contribution and local interaction is expressed from NRTL theory. A symmetric model with reference state of pure solvent and pure completely dissociated liquid electrolyte becomes basis of local interaction model development (Chen et al., 1982).

An unsymmetric model can be achieved by modeling of infinite dilution activity. Equation (3.25) is expressed as the extention of the NRTL for local interactions, the Pitzer-Debye-Hückel (PDH) model, and Born equation for enriching the excess Gibbs free energy.

Combination of long range and local contribution in ENRTL is correlated to energy interaction parameters, τ. The correlation of ENRTL and energy interaction parameters can be seen in equation from eq. (2.77) to (2.85). The excess Gibbs free energy is dependence of temperature of the system and particularly ENRTL model also consider energy interaction parameters between ionic species. The energy parameters of compound in K_2CO_3-H_2O-CO_2 system can be found in Austgen (1988).

Thermodynamic expression to calculate the activity coefficients for the ENRTL model is defined as relation between the excess Gibbs free energy and activity coefficient written below:

$$ln\gamma_i = \frac{G_m^{*E}}{RT} = \left[\frac{\delta\left(nG_m^{*E}/RT\right)}{\delta n_i}\right] \tag{3.35}$$

Applying equation (3.26) to equation (3.29) yields,

$$ln\gamma_i^* = ln\gamma_i^{*,PDH} + ln\gamma_i^{*,Born} + lni\gamma_i^{*,lc} \tag{3.36}$$

The absence of ion in equation (3.30) can reduce to the original NRTL expression for non electrolyte systems.

3.3. Flow Chart Prediction Method

Calculation model has objective to find CO_2 solubility in K_2CO_3 solution, in which parameters of ENRTL is applied. To establish with MATLAB simulation previously equation is taken and parameters for model calculation can be found in literature then should be reviewed. Parameters obtained from literature then is fitted and compared to the data from the experiments.

To find correlation of experimental data and model result, the average relative deviation should be calculated. Comparing model calculation to measured data is to make sure whether equation and parameters of model possess similar trend or not from experimental data. Fig. 3.2 shows the flow chart to predict CO_2 solubility with ENRTL model.

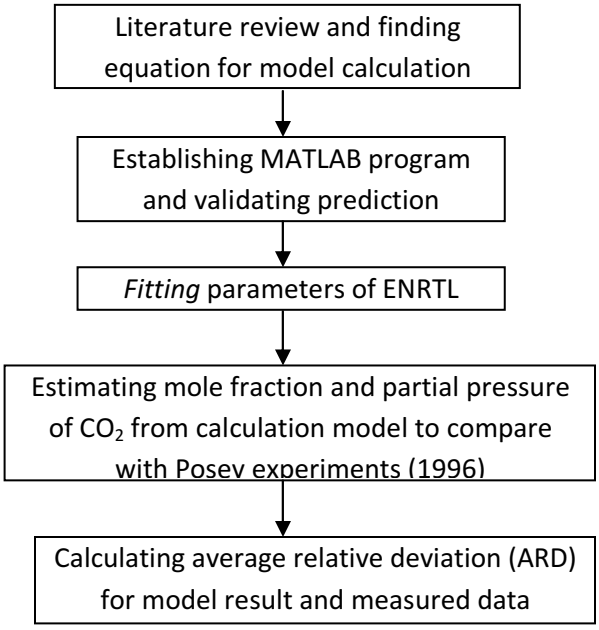

Figure 3.2 Flow chart for working method.

3.4. Algorithm for Model Estimation

MATLAB has advantage to predict data from equation and parameters of ENRTL model simultaneously, applying obtained equations from literature to MATLAB and inserting parameters into equation is the initial step to predict CO_2 solubility. Initially chemical potential standart should be found using the eq. (3.6) by forming matrices of element balances multiplied with chemical equilibrium constants of each elements then Gauss elimination was employed. After having found the chemical potential standart it is necessary to calculate the mole fraction with eq. (3.26) by setting unknown activity coefficient of any species γ_i as fixed value and also applying of Lagrange multiplier for each chemical potential . The program will calculate and iterate until the absolute difference of mole fraction species *i* at equlibrium condition and mole of CO_2 input are below the tolerance. PDH model, Born equation, and local contribution that is formulated in eq. (3.32), (3.33), and (2.73) respectively with surface and volume parameters involved is applied to find activity coefficient model. If the absolute difference of calculated and setting activity coefficient matches below the tolerance number, it will give appropriate prediction of solubility CO_2 in potassium carbonate.

Data obtained from the equation model is applied to measure CO_2 solubility, if the calculation model gives tolerance higher than absolute difference then program will repeat calculation from beginning. Conversely, when data is reached below the absolute tolerance program will continue to finish model calculation and show data from calculation. Figure 3.3 describes the algorithm of the model with ENRTL.

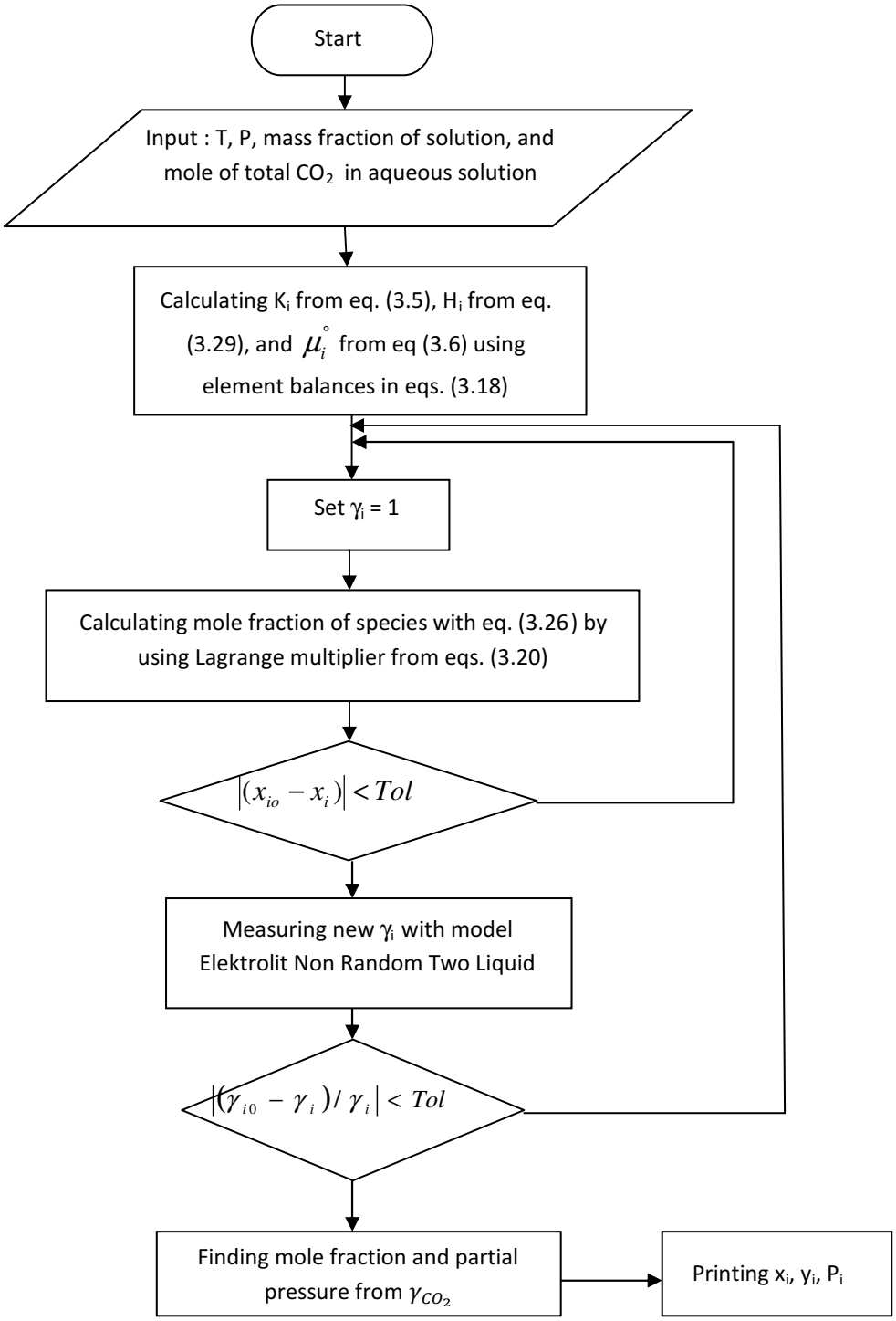

Figure 3.3 Algorithm for model estimation.

CHAPTER 4

RESULTS AND DISCUSSION

In this chapter we are going to discuss about the results of solubility of CO_2 in potassium carbonate solution at temperatures of 30, 40, 50, 70, and 90°C which are commonly used in experiments and industrial cases with ENRTL model. The pressure for prediction is kept at 1 atm, the mass of potassium carbonate is 20%, 30%, and 40% based on experiments of Posey (1996).

First, prediction program was validated using H_2O-K_2CO_3-CO_2 system with parameters of ENRTL that were taken from Austgen (1989) and calculations of Smith and Missen (1988). The interaction of parameters consists of energy, surface, and volume interactions. Predictions were compared to the experimental data of Posey (1996) for mole fraction of CO_2 in solution of potassium carbonate. After being validated program was fitted with data of energy interaction parameters which are based on the temperature range mentioned before. The results of fitted energy interaction parameters could be described in mole fractions of CO_2 in vapor phase. Solubility of CO_2 from the program is developed by MATLAB and prediction data is provided in graph as mole loading (mole of CO_2 absorbed/mole K_2CO_3 total) versus partial pressure of CO_2, because experimental data were obtained in partial pressure of each components.

4.1 Program Validation

Program validation is done to examine the accuracy of prediction of CO_2 solubility. This could be done by providing mole fraction of CO_2 loading and mole fraction prediction compared to CO_2 loading and mole fraction in K_2CO_3 solution from experimental data of Posey (1996) within percentage of K_2CO_3 mass fraction and temperature variable. ENRTL parameters used in the program are energy, surface and volume interaction parameters which are taken from Austgen (1988) of each compound. All energy interaction parameters depend on temperature. All the parameters are given in the Tables 4.1 and 4.3.

Table 4.1 Surface and Volume Interaction Parameters of H_2O-K_2CO_3-CO_2 System.

Compound	Surface (r)	Volume (Q)
CO_2	0.92	1.4
$KHCO_3^-$	0.92	1.4
K_2CO_3	4.2624	3.42
H_2O	0.92	1.4
H_3O^+	4.2624	3.42

Table 4.2 Energy Interaction Parameters of H_2O-K_2CO_3-CO_2 System.

Interaction compounds	Parameter values
H_2O – $KHCO_3$	714.14 – 2.93T
H_2O – K_2CO_3	-2477.48 + 7.56T
$KHCO_3$ – H_2O	-10926.25 – 327442.31/T
K_2CO_3 – H_2O	-554.08 + 166018.51/T
$KHCO_3$ – CO_2	-1227.43 + 0.26T
K_2CO_3 – CO_2	2827.4 + 4.45T
$KHCO_3$ – H_3O^+	4060.9 – 13.61T
K_2CO_3 – H_3O^+	-2592.34 + 9.13T
CO_2 – $KHCO_3$	138.49 – 1.38T
H_3O^+ - $KHCO_3$	152.13 – 7.99T
CO_2 – K_2CO_3	-7.27 + 1.60T
H_3O^+ - K_2CO_3	-4.68 + 1.34T

The experimental and prediction data are given in Figs. 4.1 - 4.5. Program validation shows correlation between loading of CO_2 (mole CO_2 absorbed/mole K_2CO_3 total) and mole of CO_2 in K_2CO_3 solution at liquid phase temperatures of 30, 40, 50, 70, and 90°C. Figures in this chapter are for 20%, 30%, and 40% mass K_2CO_3 which are shown as parameters.

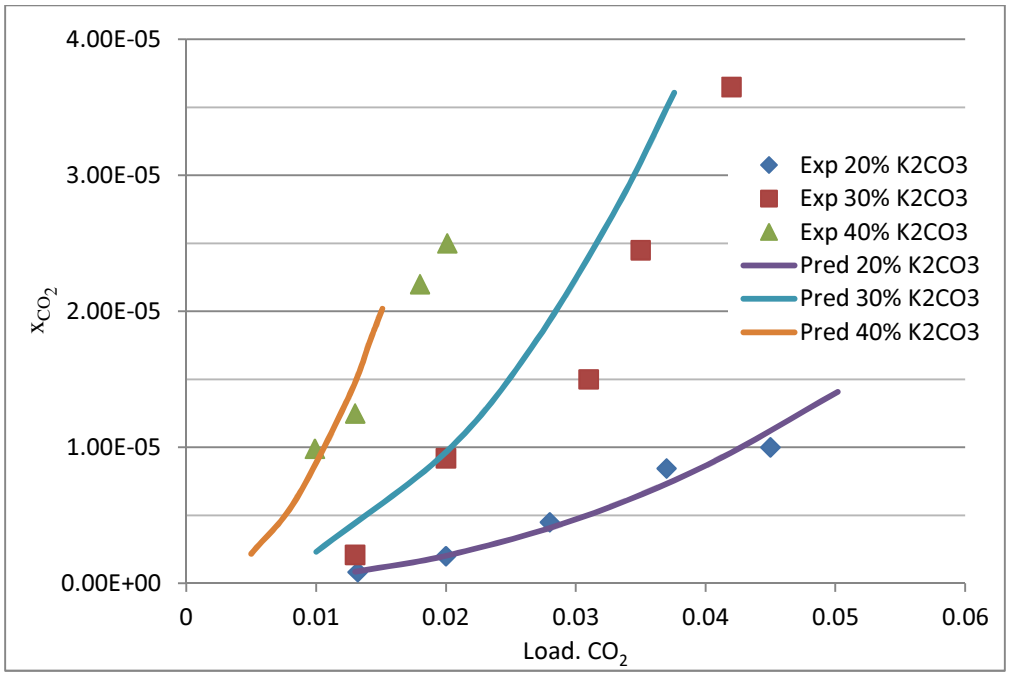

Figure 4.1 CO_2 loading vs. CO_2 mole fraction at 30°C

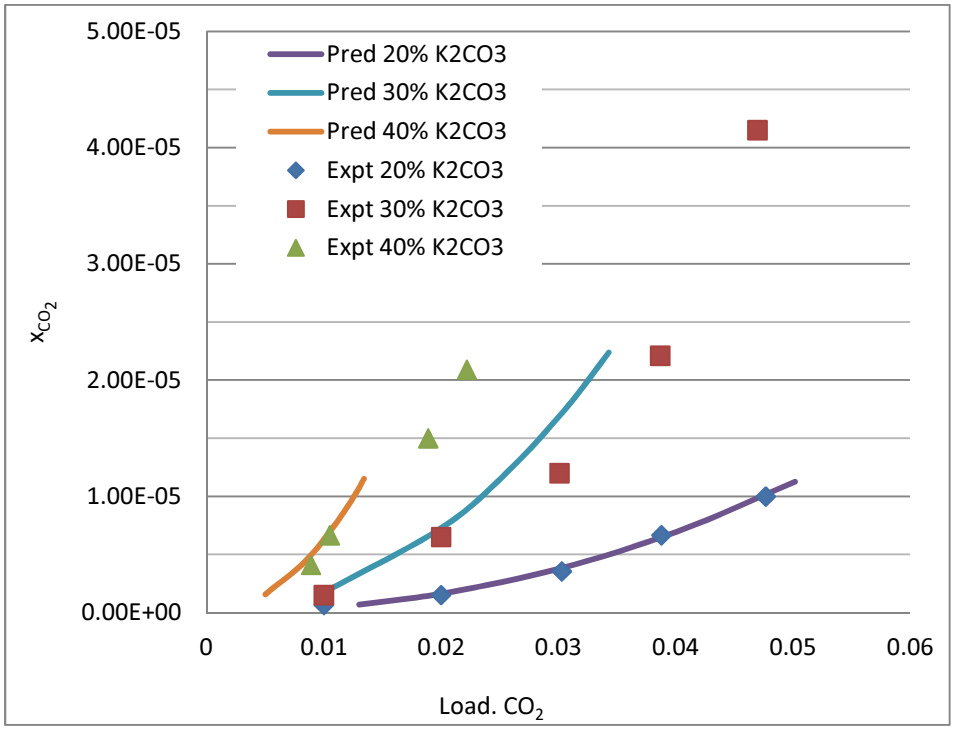

Figure 4.2 CO_2 loading vs. CO_2 mole fraction at 40°C.

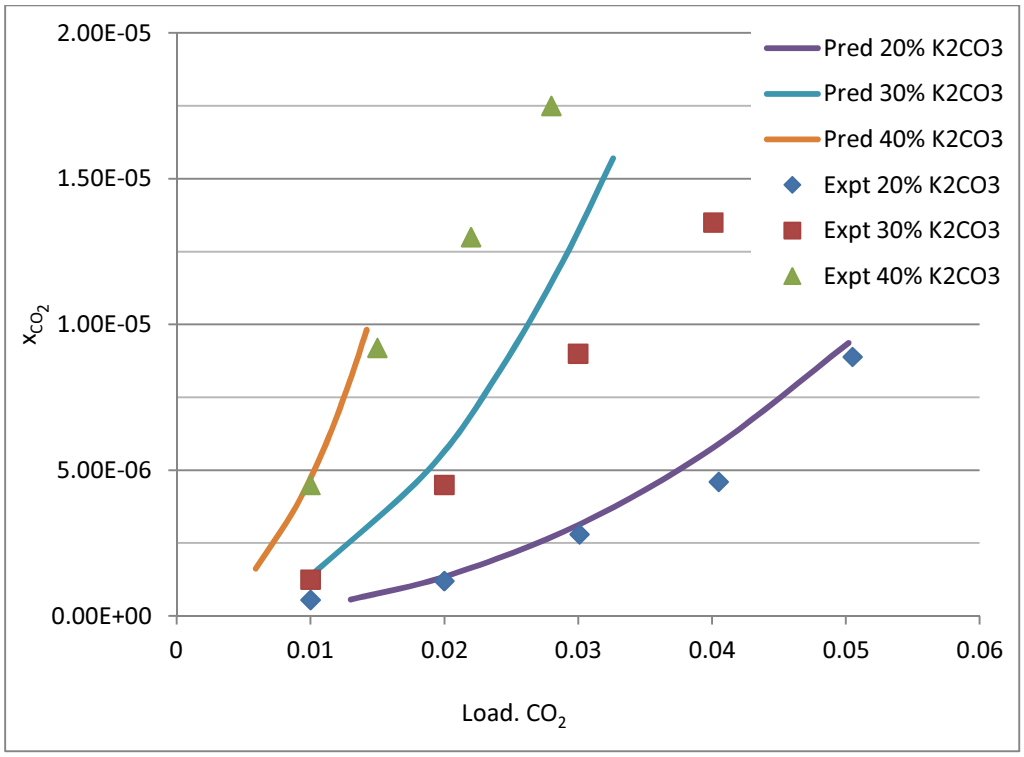

Figure 4.3 CO_2 loading vs. CO_2 mole fraction at 50°C.

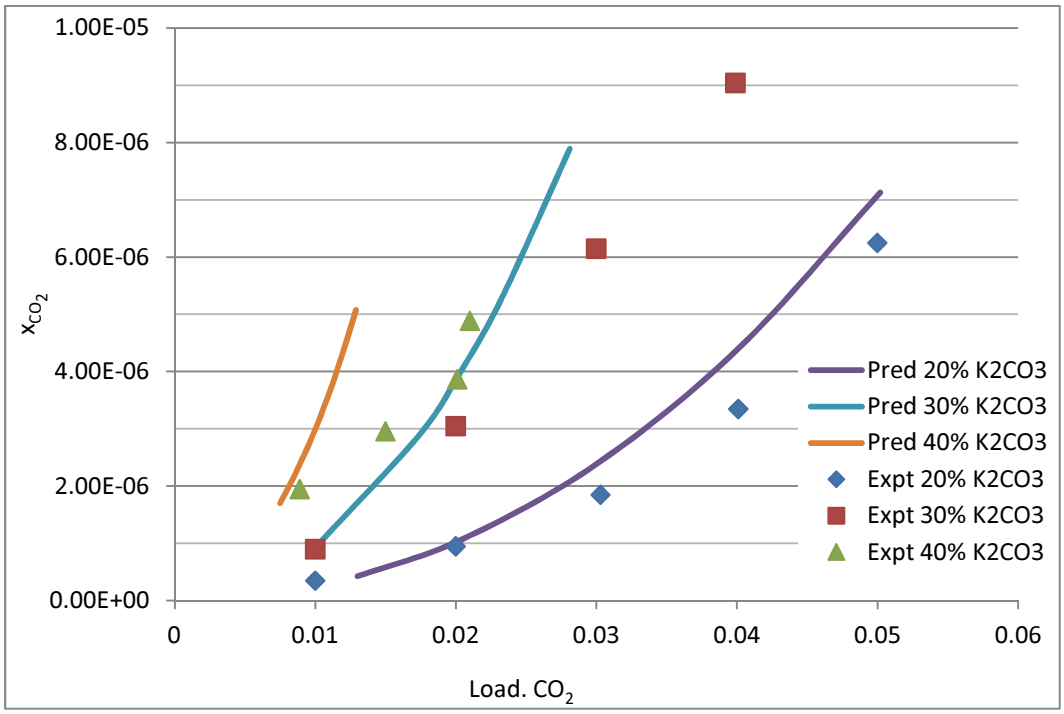

Figure 4.4 CO_2 loading vs. CO_2 mole fraction of at 70°C.

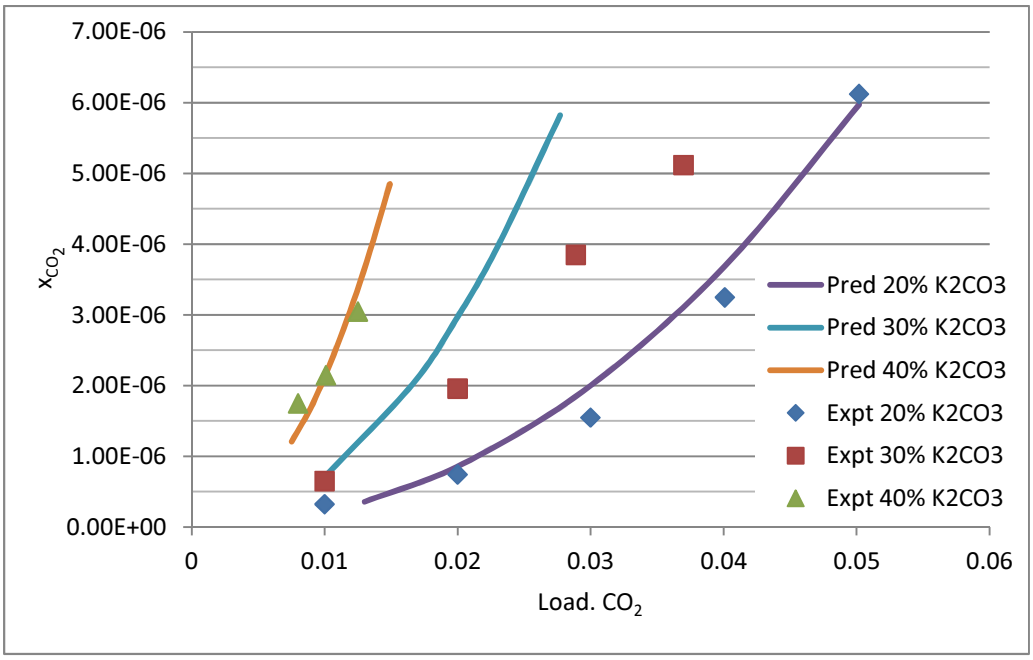

Figure 4.5 CO_2 loading vs. CO_2 mole fraction at 90°C.

As shown in the figures above, x-axis represents loading of CO_2 (mole of CO_2 absorbed/mole K_2CO_3 total) versus y-axis as mole fraction of CO_2 in liquid phase, the model calculations and experimental data give similar trends. Model calculations tend to follow experimental data when loading of CO_2 increases, so do mole fractions of CO_2 in liquid phase. Moreover, the calculation of average error by least-squares-method shows the prediction data from E-NRTL model has the minimum error range from $1{,}8.10^{-6}$ to $4{,}07.10^{-5}$. The least-squares-method can be written as:

$$\sum_1^n \left(xCO_2^{pred} - xCO_2^{expt}\right)^2 + \left(CO_2^{load,pred} - CO_2^{load,expt}\right)^2 \qquad (4.1)$$

The results of average errors from the model prediction and experimental data are provided in Table 4.3.

Table 4.3 Average Calculation Errors by Least-Squares Method.

Mass K_2CO_3 →	20 %	30 %	40 %
30 °C	8.338E-06	1.0192E-05	1.04625E-05
40 °C	3.422E-06	4.96121E-05	2.9385E-05
50 °C	1.884E-06	9.2646E-05	7.24175E-05
70 °C	1.858E-06	4.60425E-05	4.04775E-05
90 °C	1.832E-06	3.0325E-05	6.7E-07

4.2 Electrolyte Non Random Two Liquid Parameters

ENRTL parameters used for the prediction of H_2O-K_2CO_3-CO_2 system are energy interaction, surface, and volume parameters. Surface and volume parameters were given in Table 4.1 where there are twelve energy interaction parameters to be fitted by temperature dependence. The values of energy interaction parameters ware fitted until mole fraction of CO_2 in the vapor phase of the system considered give similar trends to experimental data. The energy interaction parameters fitted to temperature dependence is shown in Table 4.4 taken from Austgen (1988).

Table 4.4 Temperature fitting of ENRTL energy interaction parameters.

Interaction Compounds	**Temperature (°C)**				
	30	**40**	**50**	**70**	**90**
$\tau_{H_2O-K^+HCO_3^-}$	-174.09	-203.39	-232.69	-291.29	-349.89
$\tau_{H_2O-K^+CO_3^{2-}}$	-185.666	-110.07	-34.47	116.73	267.93
$\tau_{K^+HCO_3^--H_2O}$	-12006.4	-11971.89	-11939.53	-11880.48	-11827.92
$\tau_{K^+CO_3^{2-}-H_2O}$	-6.43524	-23.92	-40.33	-70.27	-96.92
$\tau_{K^+HCO_3^--CO_2}$	-1148.61	-1146.01	-1143.41	-1138.21	-1133.01
$\tau_{K^+CO_3^{2-}-CO_2}$	4176.418	4220.92	4265.42	4354.42	4443.42
$\tau_{K^+HCO_3^--H_3O^+}$	-64.9715	-201.07	-337.17	-609.37	-881.57
$\tau_{K^+CO_3^{2-}-H_3O^+}$	175.4195	266.72	358.02	540.62	723.22
$\tau_{CO_2-K^+HCO_3^-}$	-279.857	-293.66	-307.46	-335.06	-362.66
$\tau_{H_3O^+-K^+HCO_3^-}$	2574.299	2654.20	2734.10	2893.90	3053.70
$\tau_{CO_2-K^+CO_3^{2-}}$	477.77	493.77	509.77	541.77	573.77
$\tau_{H_3O^+-K^+CO_3^{2-}}$	401.541	414.94	428.34	455.14	481.94

Mole fraction of CO_2 in vapor phase from the calculation is interpreted as fitted E-NRTL parameters. Figures 4.6 - 4.10 show the correlation between CO_2 loading and mole fraction of

CO_2 in the vapor phase at various temperatures. The model is compared to the experimental data from Posey (1996).

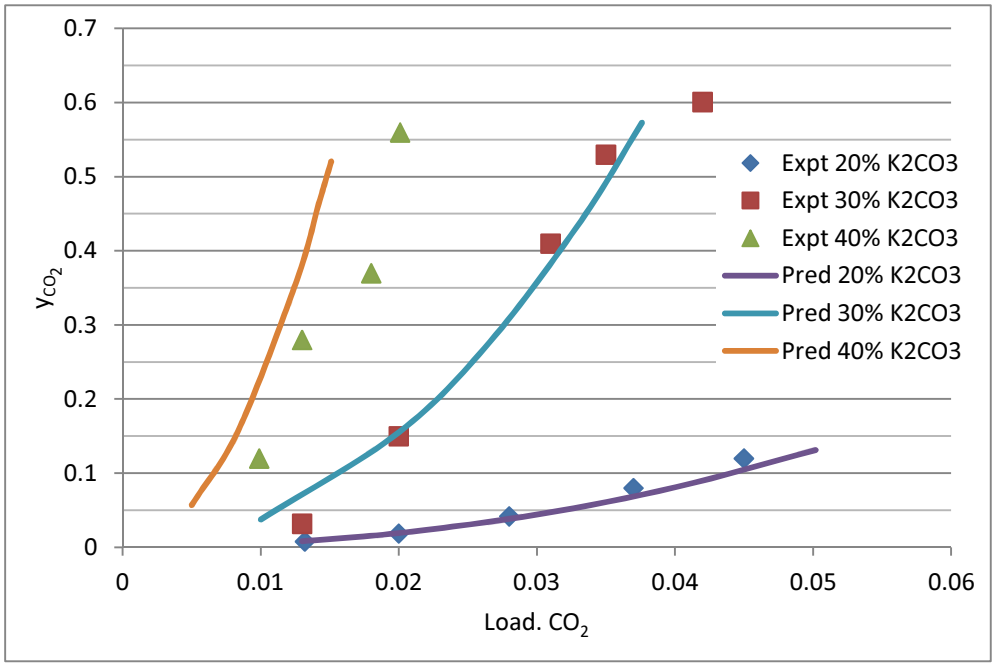

Figure 4.6 CO_2 loading vs. CO_2 mole fraction in vapor phase at 30°C.

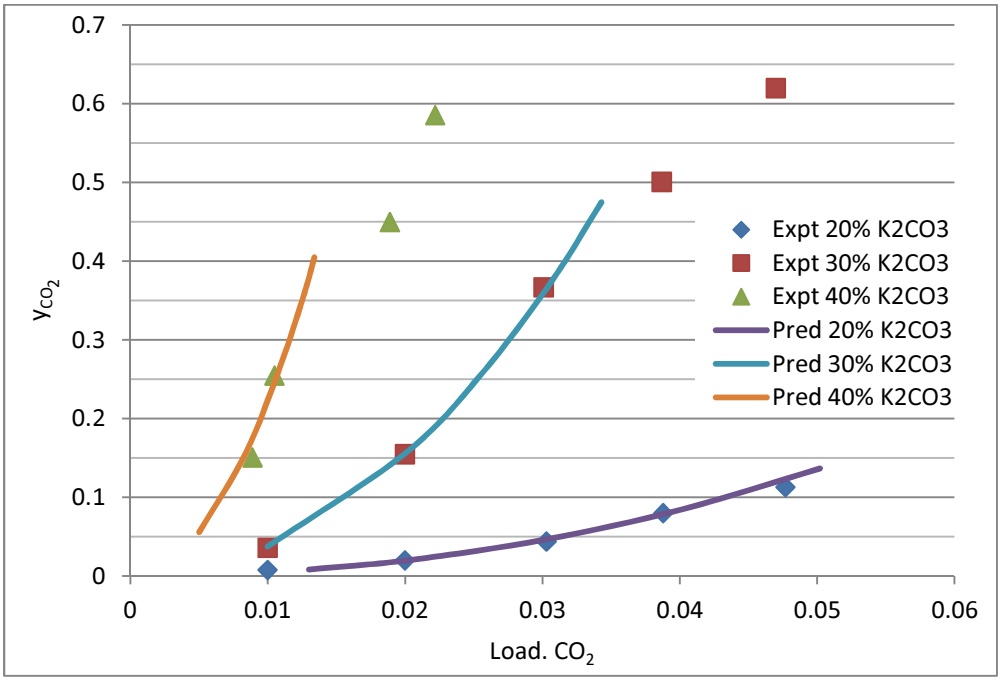

Figure 4.7 CO_2 loading vs. CO_2 mole fraction in vapor phase at 40°C.

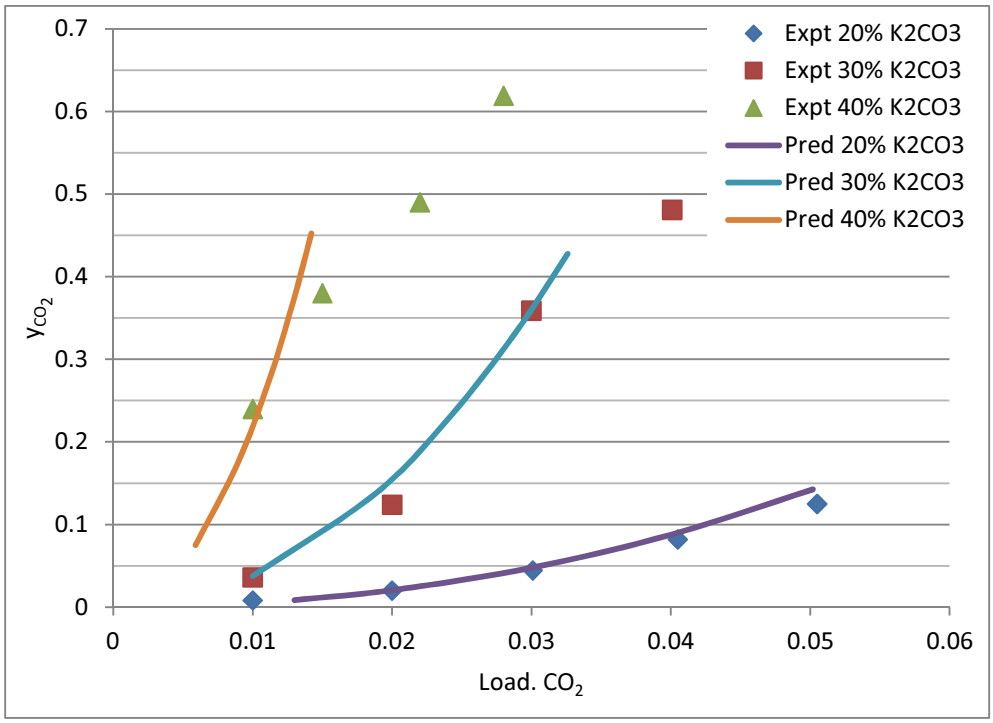

Figure 4.8 CO_2 loading vs. CO_2 mole fraction in vapor phase at 50°C.

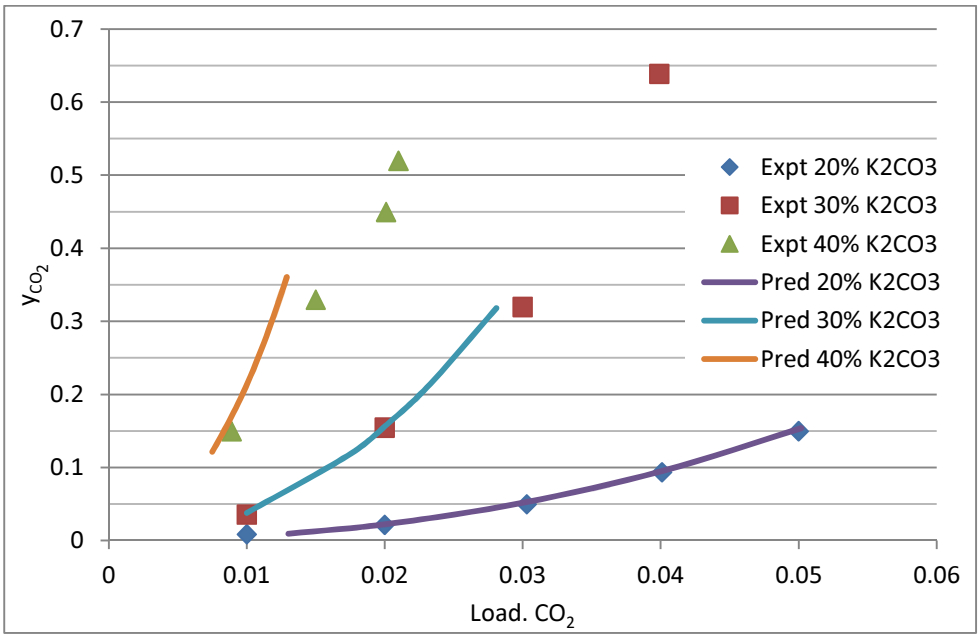

Figure 4.9 CO_2 loading vs. CO_2 mole fraction in vapor phase at 70°C.

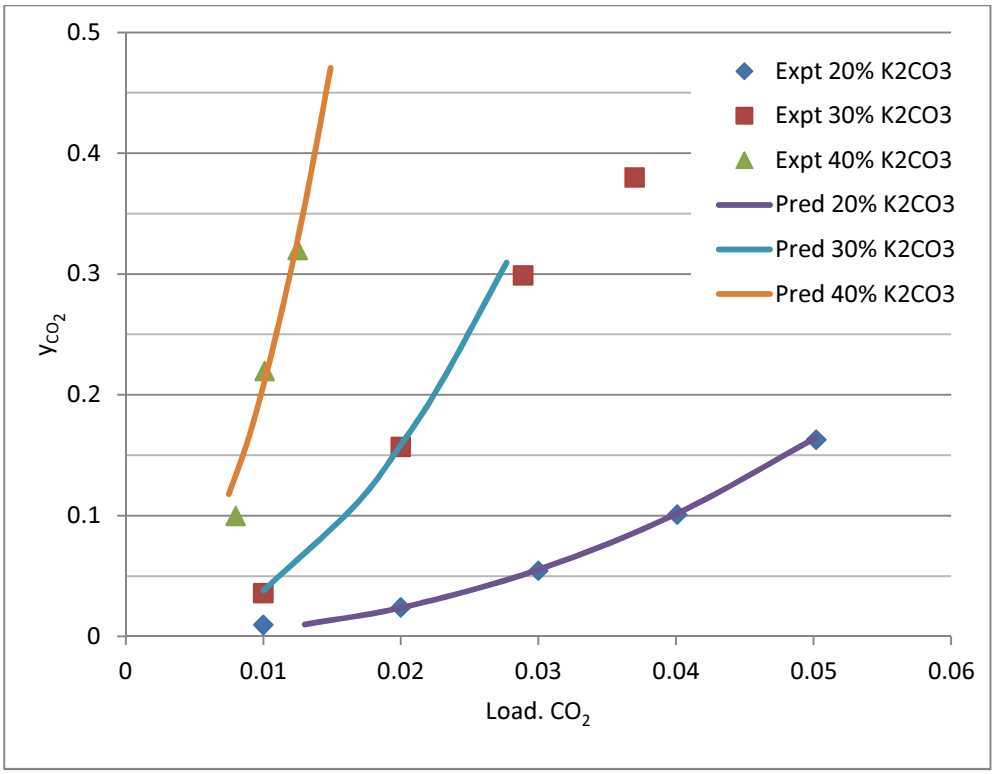

Figure 4.10 CO_2 loading vs. CO_2 mole fraction in vapor phase at 90°C.

As shown in the figures above y-axis represents mole fraction of CO_2 in vapor phase, the correlation of CO_2 loading and mole fraction of CO_2 in the vapor phase from calculation and experimental data have similar trends. It means that E-NRTL parameters taken from Austgen (1989) could be used for the prediction program, long-range forces of Pitzer-Debye-Hückel model only provide accuracy of calculation only if solution is diluted (< 1 M). In this calculation we need to know the dielectric constant as the solvent is electrolyte, the dielectric constants for water and acid species were taken from Bishnoi and Rochelle (2000).

From the figures above, it is observed that mole fraction of CO_2 increases due to increasing of electron charge especially at high temperatures. Potassium carbonate absorbs more CO_2 in conditions of higher electron charge (Bishnoi and Rochelle, 2000). Generally, industrial absorptions of CO_2 add some catalyst such as amine solution to make absorption better in terms of lower temperature and absorbent concentration.

4.3 Prediction of Solubility of CO_2

The solubility of CO_2 was measured in K_2CO_3-H_2O mixture solvent to arrive at an activity coefficient for CO_2. The solubility is an important thermodynamic parameter, defining the equilibrium concentration of the species in the liquid in the absence of chemical equilibrium. Representing the data as an activity coefficient enables the incorporation of solubility in the rigorous ENRTL framework as interaction parameters, not simply an empirical equation.

The solubility of CO_2 can be calculated based on activity coefficient with the following reason. Recall that Henry's law applies to dilute solution so that

$$P_{CO_2} = H_{CO_2}\gamma^*_{CO_2}x_{CO_2} \tag{4.2}$$

In this work, Henry's constant for pure water is dependent on temperature (Cullinane, 2005). The expression for Henry's constant is

$$H^w_{CO_2} = e^{170.7126} - \frac{8477.711}{T} - 21.95743\log T + 0.005781T \tag{4.3}$$

The solubility of CO_2 in potassium carbonate then can be represented as mole fraction of CO_2 in liquid phase and partial pressure of CO2 in vapor phase as predicted by ENRTL model using long range forces and local contribution.

Result of these calculations are presented in Tables 4.5 - 4.7 at 30°C with a range of mass percentage of potassium carbonate from 20% to 40% as used in Posey's experiments (1996). Figure 4.11 compares the results with the experimental data obtained from Posey (1996).

Table 4.5 CO_2 Solubility with 20% mass K_2CO_3 at 30°C.

CO_2 load. (exp)	CO_2 load. (pred)	P_{CO_2} exp. (kPa)	P_{CO_2} pred. (kPa)	x_{CO_2} (exp)	x_{CO_2} (pred)
0.0132	0.013	0.98	0.8043015	$8.3\text{x}10^{-7}$	$8.4\text{x}10^{-7}$
0.02	0.0204	2.01	2.0061	$2\text{x}10^{-6}$	$2.1\text{x}10^{-6}$
0.028	0.0302	4.46	4.5222	$4.5\text{x}10^{-6}$	$4.7\text{x}10^{-6}$
0.037	0.0401	8.12	8.2357	$8.45\text{x}10^{-6}$	$8.6\text{x}10^{-6}$
0.045	0.0502	12.78	13.307	10^{-5}	$1.4\text{x}10^{-5}$

Table 4.6 CO_2 Solubility with 30 % mass K_2CO_3 at 30°C.

CO_2 load. (exp)	CO_2 load. (pred)	P_{CO_2} exp. (kPa)	P_{CO_2} pred. (kPa)	x_{CO_2} (exp)	x_{CO_2} (pred)
0.013	0.01	0.98	3.78	$2.1\text{x}10^{-6}$	$2.3\text{x}10^{-6}$
0.02	0.02	2.01	15.71	$9.2\text{x}10^{-6}$	$9.6\text{x}10^{-6}$
0.03	0.0266	4.46	28.09	$1.5\text{x}10^{-5}$	$1.7\text{x}10^{-5}$
0.035	0.0332	8.12	44.67	$2.5\text{x}10^{-5}$	$2.8\text{x}10^{-5}$
0.04	0.0376	12.78	58.04	$8.6\text{x}10^{-5}$	$3.6\text{x}10^{-5}$

Table 4.7 CO_2 Solubility with 40% mass K_2CO_3 at 30°C.

CO_2 load. (exp)	CO_2 load. (pred)	P_{CO_2} exp. (kPa)	P_{CO_2} pred. (kPa)	x_{CO_2} (exp)	x_{CO_2} (pred)
0.0099	0.005	3.8	5.75	$9.9\text{x}10^{-6}$	$2.1\text{x}10^{-6}$
0.01	0.008	12.83	16.08	$1.2\text{x}10^{-5}$	$6.1\text{x}10^{-6}$
0.013	0.012	25.67	36.46	$2.2\text{x}10^{-5}$	$1.4\text{x}10^{-5}$
0.018	0.014	32.44	46.98	$2.5\text{x}10^{-5}$	$1.8\text{x}10^{-5}$
0.02	0.015	45.9	52.75	$2.9\text{x}10^{-5}$	$2\text{x}10^{-5}$

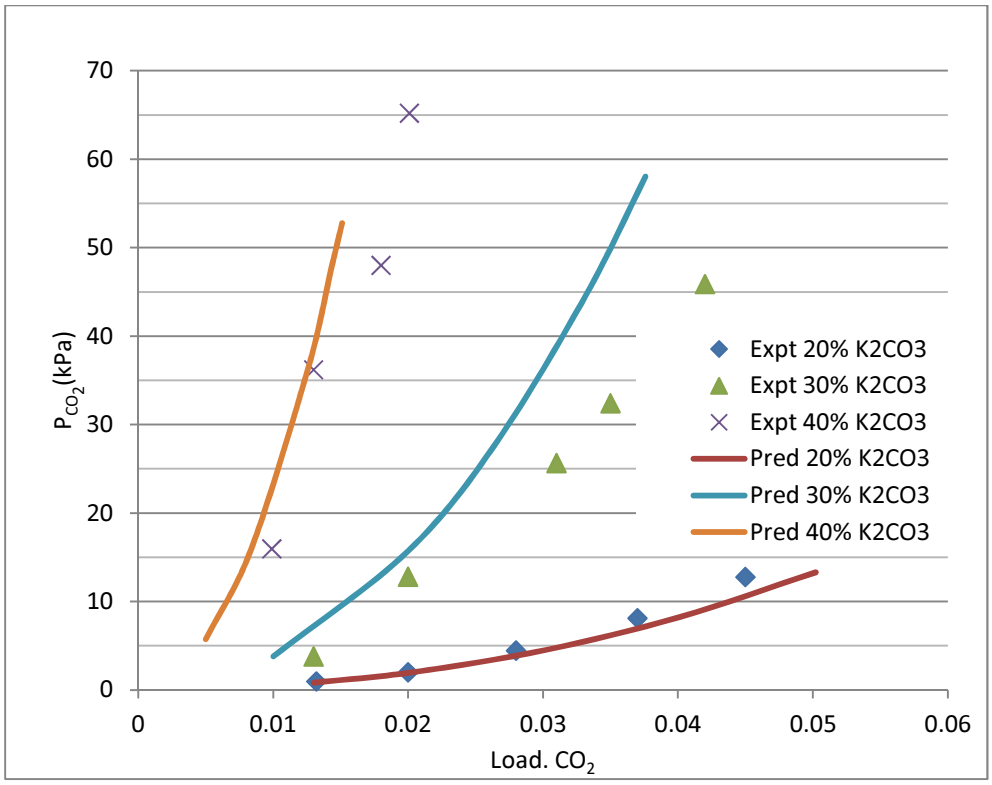

Figure 4.11 Solubility of CO_2 at 30°C and 1 atm.

From the tables above, increase of CO_2 solubility which is described as partial pressure of CO_2 in the mixture, was affected by loading of CO_2, that means concentration of K_2CO_3. The average increase of CO_2 loading range from 0.25% to 0.93% resulted in a rise of CO_2 partial pressure by about 5.7% to 31.19%. The higher concentration of K_2CO_3 increases capability of mixture solvent to absorb CO_2. Danckwerts (1972) reported that CO_2 solubility was affected by solvent concentration of K_2CO_3, pressure, and temperature condition. As for high K_2CO_3 concentration, the solubility of CO_2 also increases.

The calculation result for temperature 40°C is presented in Tables 4.8 - 4.10 respectively with the figure 4.12 as comparison data from calculation and experiments.

Table 4.8 CO_2 Solubility with 20% mass of K_2CO_3 at 40°C.

CO_2 load. (exp)	CO_2 load. (pred)	P_{CO_2} exp. (kPa)	P_{CO_2} pred. (kPa)	x_{CO_2} (exp)	x_{CO_2} (pred)
0.01	0.013	0.84	0.83	$6.5\text{x}10^{-7}$	$6.7\text{x}10^{-7}$
0.02	0.02	2.08	2.09	$1.5\text{x}10^{-6}$	$1.6\text{x}10^{-6}$
0.03	0.03	4.7	4.71	$3.5\text{x}10^{-6}$	$3.8\text{x}10^{-6}$
0.04	0.04	8.55	8.57	$6.5\text{x}10^{-6}$	$6.9\text{x}10^{-6}$
0.05	0.05	13.85	13.86	$9.9\text{x}10^{-6}$	$1.1\text{x}10^{-5}$

Table 4.9 CO_2 Solubility with 30% mass of K_2CO_3 at 40°C.

CO_2 load. (exp)	CO_2 load. (pred)	P_{CO_2} exp. (kPa)	P_{CO_2} pred. (kPa)	x_{CO_2} (exp)	x_{CO_2} (pred)
0.01	0.01	3.5	3.8	$1.5\text{x}10^{-6}$	$1.7\text{x}10^{-6}$
0.02	0.02	12.48	15.77	$6.5\text{x}10^{-6}$	$7.2\text{x}10^{-6}$
0.03	0.0255	36.77	25.85	$1.2\text{x}10^{-5}$	$1.2\text{x}10^{-5}$
0.039	0.03	45.22	37.75	$2.2\text{x}10^{-5}$	$1.7\text{x}10^{-5}$
0.042	0.034	60.89	48.11	$4.1\text{x}10^{-5}$	$2.2\text{x}10^{-5}$

Table 4.10 CO_2 Solubility with 40% mass of K_2CO_3 at 40°C.

CO_2 load. (exp)	CO_2 load. (pred)	P_{CO_2} exp. (kPa)	P_{CO_2} pred. (kPa)	x_{CO_2} (exp)	x_{CO_2} (pred)
0.0089	0.005	12.65	5.6	$4.5\text{x}10^{-6}$	$1.5\text{x}10^{-6}$
0.01	0.0084	25.01	15.8	$6.6\text{x}10^{-6}$	$4.4\text{x}10^{-6}$
0.018	0.01	34.74	26.9	$1.5\text{x}10^{-5}$	$7.5\text{x}10^{-6}$
0.02	0.012	40.09	36	$2\text{x}10^{-5}$	10^{-5}

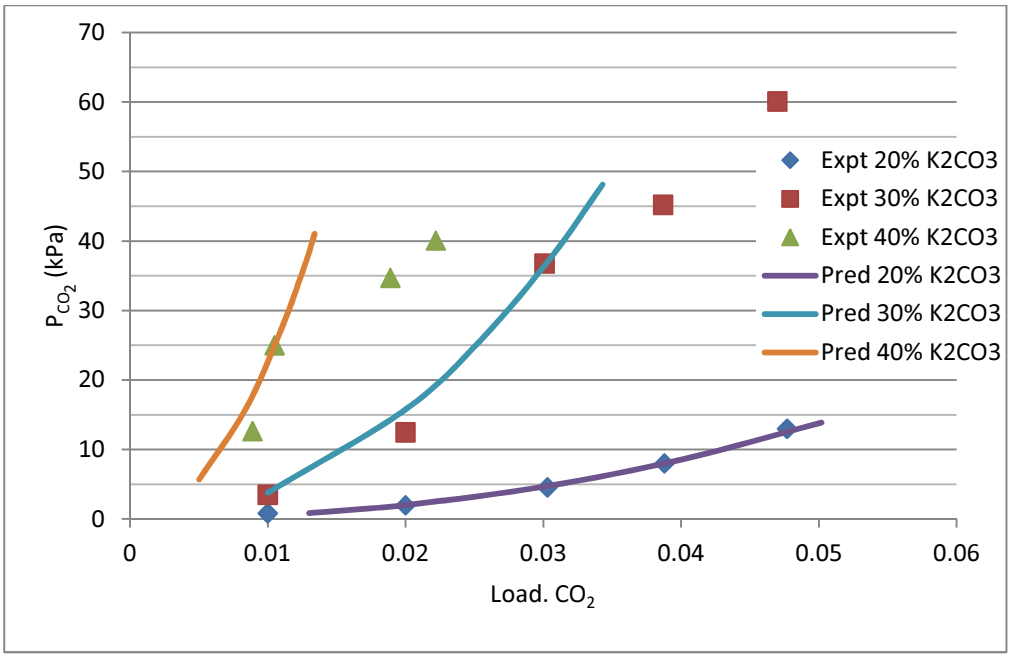

Figure 4.12 Solubility of CO_2 at 40°C and 1 atm.

With increasing of temperature, calculation models give results almost similar to the previous temperature. Partial pressure of CO_2 at 40°C with the same mass percentage increases by 5.94% to 25.91% as CO_2 loading is raised from 1.34% to 3.72%. Nevertheless, the partial pressure at 40°C reaches 4.13 % higher than partial pressure at 30°C, which means that the temperature also affects CO_2 solubility.

Results of further calculation can be seen in Tables 4.11 - 4.13 for 10°C higher than previous calculations. Fig. 4.13 presents comparison of calculated and experimental data.

Table 4.11 CO_2 Solubility with 20% mass K_2CO_3 at 50°C.

CO_2 load. (exp)	CO_2 load. (pred)	P_{CO_2} exp. (kPa)	P_{CO_2} pred. (kPa)	x_{CO_2} (exp)	x_{CO_2} (pred)
0.01	0.013	0.76	0.87	$5.5\text{x}10^{-7}$	$5.6\text{x}10^{-7}$
0.02	0.02	2.01	2.17	$1.2\text{x}10^{-6}$	$1.4\text{x}10^{-6}$
0.03	0.03	4.59	4.9	$2.8\text{x}10^{-5}$	$3.1\text{x}10^{-6}$
0.04	0.04	8.61	8.93	$4.6\text{x}10^{-5}$	$5.8\text{x}10^{-6}$
0.05	0.05	12.33	14.44	$8.9\text{x}10^{-5}$	$9.3\text{x}10^{-6}$

Table 4.12 CO_2 Solubility with 30% mass K_2CO_3 at 50°C.

CO_2 load. (exp)	CO_2 load. (pred)	P_{CO_2} exp. (kPa)	P_{CO_2} pred. (kPa)	x_{CO_2} (exp)	x_{CO_2} (pred)
0.01	0.01	3.51	3.8	$1.25\text{x}10^{-6}$	$1.4\text{x}10^{-6}$
0.02	0.018	12.28	13.92	$4.5\text{x}10^{-6}$	$5\text{x}10^{-6}$
0.028	0.024	24.89	23.25	$9\text{x}10^{-6}$	$8.4\text{x}10^{-6}$
0.034	0.028	38.43	33.51	$1.3\text{x}10^{-5}$	$1.2\text{x}10^{-5}$
0.039	0.032	50.79	43.32	$1.8\text{x}10^{-5}$	$1.6\text{x}10^{-5}$

Table 4.13 CO_2 Solubility with 40% mass K_2CO_3 at 50°C.

CO_2 load. (exp)	CO_2 load. (pred)	P_{CO_2} exp. (kPa)	P_{CO_2} pred. (kPa)	x_{CO_2} (exp)	x_{CO_2} (pred)
0.01	0.005	12.45	7.6	$4.5\text{x}10^{-6}$	$1.6\text{x}10^{-6}$
0.015	0.0084	20.99	17.5	$9.2\text{x}10^{-6}$	$5.8\text{x}10^{-6}$
0.02	0.01	32.71	27.4	$1.3\text{x}10^{-5}$	$8\text{x}10^{-6}$
0.022	0.012	46.22	45.84	$1.8\text{x}10^{-5}$	$9.8\text{x}10^{-6}$

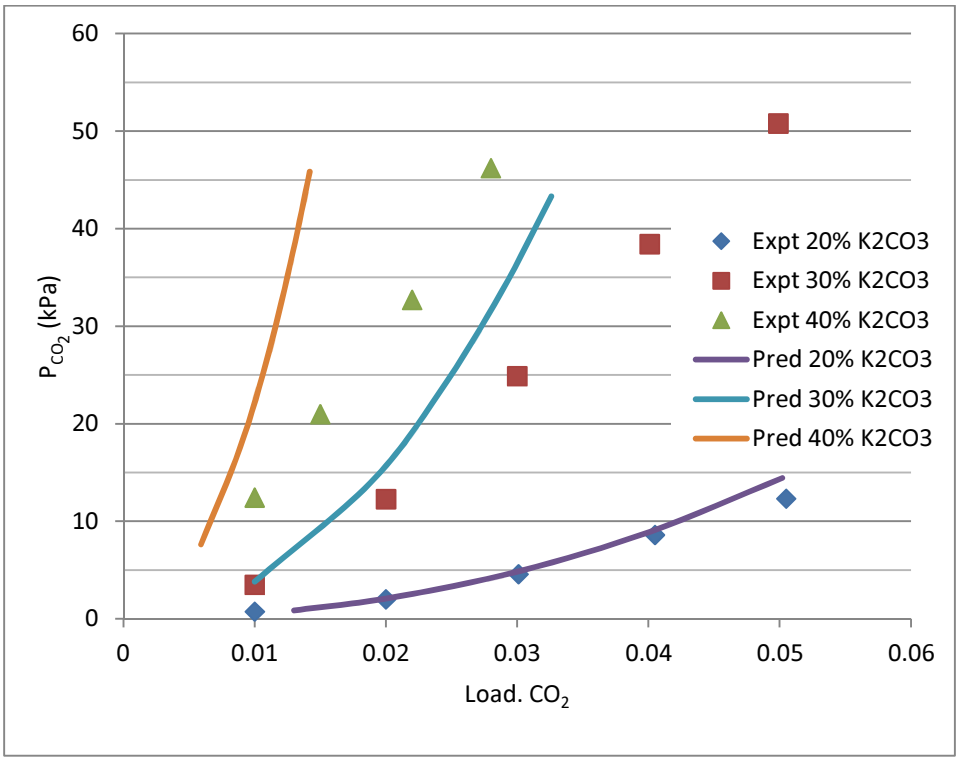

Figure 4.13 Solubility of CO_2 at 50°C and 1 atm.

The calculated results at 50°C provide higher level of partial pressure compared to the previous temperature by about 4.15%. The raise of temperature obviously affects CO_2 solubility in K_2CO_3 solution. For industrial cases with K_2CO_3 as absorbent to reduce CO_2 concentration in gas mixture optimum temperature operation reaches 50-90°C (Centola and Tellini, 2010). While the loading of CO_2 increases about 1.42%- 5.02% the partial pressure of CO_2 at 50°C increases 6.18% to 26.84%.

Tables 4.14 - 4.16 show calculated results at 70°C to place on par with Posey's experiments (1996). Figure 4.14 also compares calculated and experimental data.

Table 4.14 CO_2 solubility with 20% mass K_2CO_3 at 70°C.

CO_2 load. (exp)	CO_2 load. (pred)	P_{CO_2} exp. (kPa)	P_{CO_2} pred. (kPa)	x_{CO_2} (exp)	x_{CO_2} (pred)
0.01	0.013	0.81	0.94	$3.5\text{x}10^{-7}$	$4.3\text{x}10^{-7}$
0.02	0.02	2.08	2.34	$9.5\text{x}10^{-7}$	$1.1\text{x}10^{-6}$
0.03	0.03	5.11	5.23	$1.8\text{x}10^{-6}$	$2.4\text{x}10^{-6}$
0.04	0.0401	8.99	9.64	$3.3\text{x}10^{-6}$	$4.4\text{x}10^{-6}$
0.05	0.0502	15.52	15.59	$6.2\text{x}10^{-6}$	$7.1\text{x}10^{-6}$

Table 4.15 CO_2 solubility with 30 % mass K_2CO_3 at 70°C.

CO_2 load. (exp)	CO_2 load. (pred)	P_{CO_2} exp. (kPa)	P_{CO_2} pred. (kPa)	x_{CO_2} (exp)	x_{CO_2} (pred)
0.01	0.01	3.53	3.8	$9\text{x}10^{-7}$	$9.3\text{x}10^{-7}$
0.02	0.02	9.98	11.77	$3\text{x}10^{-6}$	$2.8\text{x}10^{-6}$
0.03	0.029	22.64	16.17	$6.1\text{x}10^{-6}$	$3.9\text{x}10^{-6}$
0.04	0.038	38.11	32.22	$9\text{x}10^{-6}$	$7.8\text{x}10^{-6}$

Table 4.16 CO_2 solubility with 40 % mass of K_2CO_3 at 70°C.

CO_2 load. (exp)	CO_2 load. (pred)	P_{CO_2} exp. (kPa)	P_{CO_2} pred. (kPa)	x_{CO_2} (exp)	x_{CO_2} (pred)
0.0089	0.0075	12.35	12.29	$1.9\text{x}10^{-6}$	$1.7\text{x}10^{-6}$
0.015	0.0087	20.41	16.46	$2.9\text{x}10^{-6}$	$2.2\text{x}10^{-6}$
0.02	0.01	32.63	22.03	$3.8\text{x}10^{-6}$	$3.1\text{x}10^{-6}$
0.021	0.013	38.04	36.52	$4.9\text{x}10^{-6}$	$5.1\text{x}10^{-6}$

The higher temperature for calculation shows increasing of partial pressure wider than previous range. At 70°C, partial pressure of CO_2 rose by 7.76% in comparison to the previous calculations; when the range is within 10°C the calculation model gives about only 4% rise of partial pressure. Steinar (2001) stated that CO_2 is well absorbed at temperatures of 70-80°C, especially for removing CO_2 from natural gas. The ENRTL model describes the data well throughout the range of concentration.

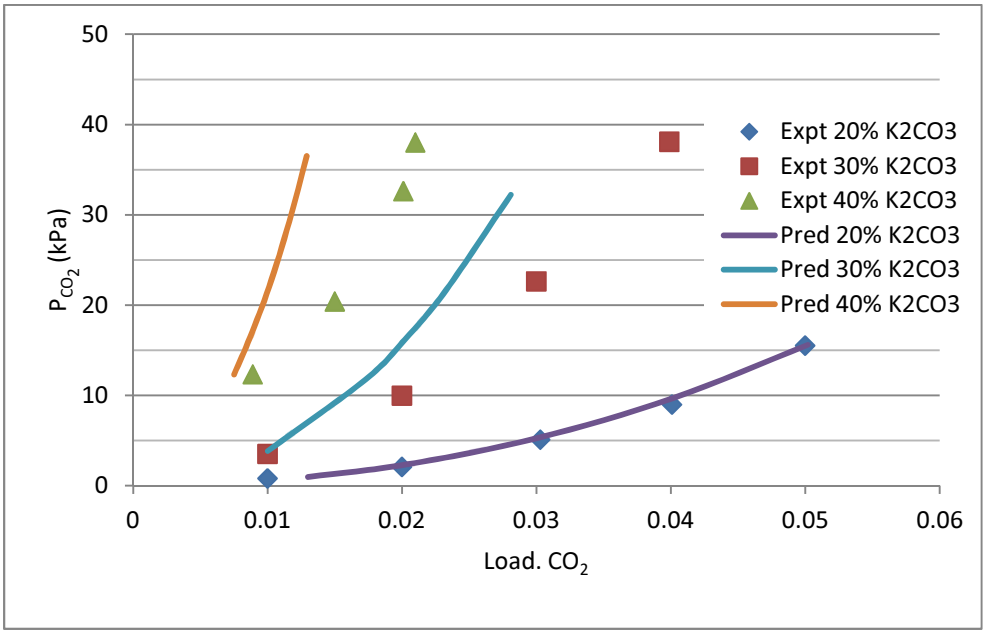

Figure 4.14 Solubility of CO_2 at 70°C and 1 atm.

As shown in the table, rise of CO_2 partial pressure varied between 6.67% and 23% at 70°C along with increasing of CO_2 loading from 1.29% to 5.02%. From Fig. 4.16 calculation models tend to indicate higher values from experimental data in particular at high concentration of solution. It is clear that at high concentrations and temperature, solution ion, HCO_3^-, possesses bigger ionic strength eventually having a significant impact on γ_{CO_2}. Measurement in K_2CO_3 closely matched the model of Weisenberger and Schumpe (1996), at a constant ionic strength the activity coefficient increases as K_2CO_3 is replaced with $KHCO_3$. Even though the solubility in $KHCO_3$ is quite difficult to measure experimentally, the model estimation still is consistent with measured data and gives a higher γ_{CO_2} (Cullinane, 2005).

Last calculation for ENRTL model is conducted at 90°C, because with the 40% mass K_2CO_3, solution is near at its boiling point, 107°C. It was also studied by Tosh et al. (1959) and Benson et al. (1954) and reported that CO_2 would be soluble in K_2CO_3 only if bicarbonate conversion reached 80-90% but not outside this range. When absorber operates at higher temperatures but constant pressure, there is not sufficient driving force in the absorber for transfer of CO_2 from the gas phase to the liquid phase. The process should be operated at higher pressures so that desorption of CO_2 can take place in the absorber (Anusha, 2010).

Tables 4.17-4.19 present results of model calculation at 90 °C and Fig. 4.15 shows the comparison with experimental data.

Table 4.17 CO_2 solubility with 20% mass K_2CO_3 at 90°C.

CO_2 load. (exp)	CO_2 load. (pred)	P_{CO_2} exp. (kPa)	P_{CO_2} pred. (kPa)	x_{CO_2} (exp)	x_{CO_2} (pred)
0.01	0.013	0.99	1.01	3.2×10^{-7}	3.6×10^{-7}
0.02	0.02	2.1	2.51	7.5×10^{-7}	8.9×10^{-7}
0.03	0.03	5.29	5.6	1.5×10^{-6}	2×10^{-6}
0.04	0.0401	9.97	10.31	3.2×10^{-6}	3.6×10^{-6}
0.05	0.0502	15.44	16.67	5.5×10^{-6}	5.9×10^{-6}

Table 4.18 CO_2 solubility with 30% mass K_2CO_3 at 90°C.

CO_2 load. (exp)	CO_2 load. (pred)	P_{CO_2} exp. (kPa)	P_{CO_2} pred. (kPa)	x_{CO_2} (exp)	x_{CO_2} (pred)
0.01	0.01	3.59	3.8	6.5×10^{-7}	7.1×10^{-7}
0.02	0.016	12.72	10.92	1.9×10^{-6}	2×10^{-6}
0.028	0.023	32.07	21.4	3.8×10^{-6}	3.9×10^{-6}
0.035	0.027	40.14	31.35	5.1×10^{-6}	5.8×10^{-6}

Table 4.19 CO_2 solubility with 40% mass K_2CO_3 at 90°C.

CO_2 load. (exp)	CO_2 load. (pred)	P_{CO_2} exp. (kPa)	P_{CO_2} pred. (kPa)	x_{CO_2} (exp)	x_{CO_2} (pred)
0.008	0.0075	10.1	11.93	1.7×10^{-6}	1.2×10^{-6}
0.01	0.01	20.59	25.14	2.1×10^{-6}	2.5×10^{-6}
0.012	0.012	32.66	35.48	3.2×10^{-6}	4.8×10^{-6}

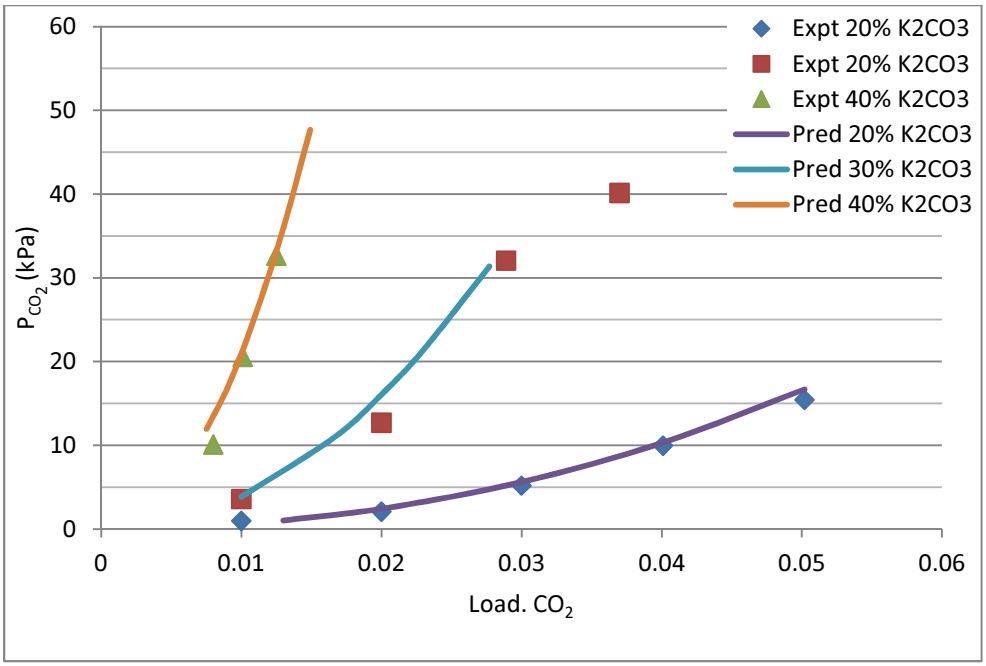

Figure 4.15 Solubility of CO_2 at 90°C and 1 atm.

As shown in Figs. 4.11 to 4.15 with y-axis represents partial pressure of CO_2, it is interesting to note that some of the form model correlation is somehow different from experimental trends, leading to systematic errors. As noted by Cullinane (2005) that temperature has an effect on interaction parameter. Chen et al. (1982) also noted that the greater the absolute value of the difference in interaction parameters for a molecule-ion pair (Example: $\left|\tau_{H_2OK^+CO_3^{2-}} - \tau_{K^+CO_3^{2-}H_2O}\right|$) would give also the greater the association of the ion pair. A lower degree of association between the ion pair at higher temperatures is expected, thus the molecule-ion pair parameters should have positive temperature dependence. This trend is found in the present calculation as well. Yet, the ENRTL model used in CO_2 solubility prediction represents the data set using only molecule-ion parameters particularly in local contribution with binary interaction between potassium carbonate and water, it resulted deviation the measured data from experimental.

Some figures shows that model calculation data reached maximum marks lower than experimental data, activity coefficient of ENRTL used in calculation based on Pitzer-Debye-Hückel, Born equation, and long range contribution has impact on constant pressure. Effect of

constant pressure gives lower range Gibbs excess energy resulting lower activity coefficient model as studied. Recalling equation from Chen *et al.* (1979) to describe prediction of CO_2 solubility from Heny's constant is written below.

$$P_{CO_2} = x_{CO_2} \gamma_{CO_2} H_{CO_2} \tag{4.4}$$

Pressure has impacts for solubility of carbon dioxide in electrolyte solution hence lower pressure solubility tends to decrease. ENRTL calculated activity coefficient of ionic species in equilibrium constant, the activity coefficient of CO_2 increases along with CO_2 loading (mole CO_2 absorbed/ mole K_2CO_3 total) but in other side mixed electrolyte solution system decreases even two or three more lower than vapor species. It explained ENRTL effect of pressure, constant pressure gave wide range increasing of activity coefficient in vapor species but within different pressure activity coefficient will give more variation range of activity coefficient result (Wilson, 1964).

The average relative deviation (ARD) of calculation models compared to the experimental data is presented in Table 4.20.

Table 4.20 Average Relative Deviation of Model Calculation.

Average Relative Deviation			
	K_2CO_3 % mass		
Temperature (°C)	20	30	40
30	5.01%	7.18%	5.67%
40	4.81%	8.68%	9.76%
50	10.34%	11.25%	11.06%
70	7.90%	11.55%	11.11%
90	8.14%	11.45%	11.07%

Table 4.20 shows that average relative deviation of model from this work varies of K_2CO_3 mass fraction and temperature. Overall the range of deviation is in the range 5% - 12%.

CHAPTER V

CONCLUSION

Result from this work showed that model of ENRTL through simulation by MATLAB using ion parameters from Pitzer-Debye-Hückel (PDH), Born equation, and local contribution Gibbs excess energy gave an optimum data set for CO_2 solubility prediction for H_2O-K_2CO_3-CO_2 system. The model can be obtained by representating mole fraction and partial pressure of CO_2 prediction. ENRTL model was used to predict activity coefficient (γ_{CO_2}) as a part of calculating partial pressure CO_2 with potassium carbonate aqueous solution in equilibrium condition at temperature 30°C, 40°C, 50°C, 70°C, and 90°C with range from $6.7x10^{-6}$ – $9.26x10^{-3}$% error.

The model of ENRTL is able to represent solubility data with average relative deviation (ARD) range from 5% to 12%. The lower ARD was found at temperature 30°C and potassium carbonate 20% mass fraction. However most of the high errors have been identified in higher temperature of calculations particularly in 70° and 90°C and the potassium carbonate solution with 40% mass fraction. The ENRTL calculation for future work suggests refining the interaction parameters specified to short-range forces which involve excess Gibbs free energy of mixed non electrolyte solution.

NOTATIONS

a : activity

D : dielectric constant

e : electron charge

f : fugacity (Pa)

Δf : fugacity diferential

G : Gibbs free energy (J/mol)

g : Gibbs excess free energy (J/mol)

$\bar{g}$: partial molar Gibbs free energy (J/mol)

H_i : Henry's constant

H : entalphy

I : ionic strength (mol/dm^3)

K : equilibrium constant

Load. : Loading

MEA : monoethanolamine

MW : molecular weight

m : molality (mol/g)

n : mole

N_A : Avogadro Number (6.02214129x10^{23}/mol)

P : pressure (Pa)

PZ : piperazine

q : spherical molecule

R : ideal gas constant (J /mole K)

S : entropy (J/K)

T : temperature (K)

U : internal energy (J)

v : molar volume (dm^3/mol)

V : volume (dm^3)

VLE : vapor liquid equilibrium

X : effective local mole fraction

x : mole fraction in liquid phase

y : mole fraction in vapor phase

z : ionic valence

Greek notation

β : interaction coefficient

γ : activity coefficient

Γ : potential energy of ion or molecule interaction

Γ_i : integration constant

ε : absolute permittivity

κ : Debye length

λ : Lagrangian multiplier

Λ : ion interaction

μ : chemical potential

π : phase

$\prod$: total

τ : interaction parameter

ξ : volume fraction

ρ : density (g/dm^3)

Subscripts

α : randomness parameter

Am : infinite dilution

Amine : amine solution

Born : Born

CO_2 : Carbon Dioxide

i,j,k : species counter

LR : long range

m : molality

MX : completely dissociated

NRTL : Non Random Two Liquid

PDH : Pitzer-Debye-Hückel

SR : short range

w : water

x : mole fraction

+ : cation

- : anion

$\underline{\pm}$: mean values

Superscripts

aq : aqueous phase

Cc : combination

E : excess in capital

ex : excess

id : ideal

ig : ideal gas

l : liquid phase

m : molality

M : mixed

tot : total

v : vapor phase

* : asymmetric

∞ : infinite

REFERENCES

1. Anusha, K., *Carbon Dioxide Capture by Chemical Absorption: A Solvent Comparison Study*. Doctor of Philosophy Dissertation: Massachusetts Institute of Technology, 2010.
2. Apelblat, A., *The vapor pressure of water over saturated aqueous solution of barium chloride, magnesium nitrate, calcium nitrate, potassium carbonate, and zinc sulfate at temperature from 283 K to 313 K*. Journal of Chemical Thermodynamics **24**, 1982, 619-626.
3. Archer, D.G., *Journal of Physical Chemistry*. Reference Data **22**(6), 1993, 1441-1453.
4. Aseyev, G.G. and Zaytsev, I.D., *Volumetric Properties of Electrolyte Solution: Estimation Method and Experimental Data*. Begell House: New York, 1996.
5. Aseyev, G.G., *Electrolytes: Equilibria in Solutions, Calculation of Multicomponent Systems, and Experimental Data on the Activities of Water, Vapor Pressure, and Osmotic Coefficients*. Begel House: New York, 1999.
6. Astarita, G., Bisio, A. and Savage, D.W., *Gas treating with Chemical Solvents*. John Willey and Sons: New York, 1983.
7. Atkins, P. and de Paula, J., *Physical Chemistry, 7th ed.*. WH Freeman Company: New York, 2002.
8. Austgen, D.M. and Smith, A.K., *Thermodynamics of Carbon Dioxide and Alkanolamines in Aqueous and non-Aqueous Solution Systems*. Chemical Engineering Science, **43**, 1988, 575-589.
9. Austgen, D.M., *A Model for Vapor-Liquid Equilibrium for Acid Gas-Alkanolamine-Water System*. Doctor of Philosophy Dissertation: University of Texas at Austin, 1988.
10. Austgen, D.M., G.T. Rochelle, Peng, X. and Chen, D.C., *Model of Vapor-Liquid Equilibria for Aqueous Acid Gas-Alkanolamine Systems Using the Electrolyte-NRTL Equation*. Ind. Eng. Chem. Res. **28**, 1989, 1060-1073.
11. Bartoo, R.K., *Removing Acid Gas by the Benfield Process*. Chemical Engineering Progress **80**(10), 1984, 35-39.
12. Benson, H.E., Field, J.H. and Jimeson, R.M., *Carbon Dioxide Absorption Employing Hot Potassium Carbonate Solution*. Chemical Engineering Progress **50**, 1954, 356-364.

13. Bishnoi, S. and Rochelle, G. T., *Absorption of Carbon Dioxide in Aqueous Piperazine/Methyldietanolamine*. AIChE Journal **48**(12), 2002, 2788-2799.
14. Bishnoi, S. and Rochelle, G. T., *Physical and Chemical Solubility of Carbon Dioxide in Aqueous Methyldietanolamine*. Fluid Phase Equilibria **168**, 2000, 214-258.
15. Bromley, L.A., *Thermodynamics Properties of Strong Electrolytes in Aqueous Solutions*. AIChE Journal **19**(2), 1973, 313-320.
16. Centola, P. and Tellini, M., *Low Pressure CO_2 Absorption from Flue Gas.* Hydrocarbon Processing Magazine, April 2011, 69-77.
17. Chapel, D. and Ernest, J., *Recovery of Carbon Dioxide from Flue Gases: Commercial Trends*. Canadian Chem. Engineering Society Presentation. October 4-6(340), 1999.
18. Chen, C. and Mathias, P.M.. *Applied Thermodynamics for Process Modeling*. AIChE Journal **48**(2), 2002, 194-199.
19. Chen, C., Britt, H.I., Boston, J.F. and Evans, L.B., *Extension and Application of the Pitzer Equation for Vapor-Liquid Equilibrium of Aqueous Electrolyte Systems with Molecular Solutes*. AIChE Journal **25**(5), 1979, 820-831.
20. Chen, C. Britt, H.I. Boston, J.F. and Evans, L.B., *Local Composition Model of Excess Gibbs Energy for Electrolyte System. Part I: Single Solvent, Single Completely Dissociated Electrolyte Systems*. AIChE Journal **28**(4), 1982, 588-596.
21. Chen, C., Mock B., and L.B. Evans, *A Local Composition Model for the Excess Gibss Energy of Aqueous Electrolyte Systems*. AIChE Journal **32**(3), 1986, 444-454.
22. *CRC Databook of Chemistry and Physics*. CRC Press: New York, 2000.
23. Cullinane, J.T. and Rochelle, G.T., *Thermodynamics of Aqueous Potassium Carbonate, Piperazine, and Carbon Dioxide Mixtures*. Fluid Phase Equilibrium **227**(2), 2004, 197-213.
24. Cullinane, J.T., *Carbon Dioxide Absorption in Aqueous Mixture of Potassium Carbonate and Piperazine*. M. S. Thesis: The University of Texas at Austin, 2002.
25. Cullinane, J.T., *Thermodynamics and Kinetics of Aqueous Piperazine with Potassium Carbonate for Carbon Dioxide Absorption*. Doctor of Philosophy Dissertation: The University of Texas at Austin, 2005.
26. Danckwerts, P.V. and Sharma, M.M., *Absorption of Carbon Dioxide into Solutions of Alkalies and Amines*. Chemical Engineering **20**(22), 1966, 244-280.

27. Danckwerts, P.V., *Significance of Liquid-Film Coefficients in Gas Absorption*. Ind. Eng. Chem. Res. **43**(13), 1951, 1460-1467.
28. Danckwerts, P.V., *The Absorption of Gas in Liquids*. Chemical Engineering Dept. Cambridge University Press: United Kingdom, 1972.
29. Debye, P. and Hückel, E., *Zur Theorie der Elekrolyte: I. Gefrierpunktserniedrigung und verwandte Erscheinungen*. Physikalische Zeitschrift, **24**(9), 1923, 185-206.
30. Deshmukh, R.D. and Mather, A.E., *A Mathematical Model for Equilibrium Solubility of Hydrogen Sulfide and Carbon Dioxide in an Aqueous Alkanolamine Solution*. Chemical Engineering Science, **36**, 1981, 355-362.
31. Edwards, T.J., Maurer, G., Newman, J. and Prausnitz, J.M., *Thermodynamics of Aqueous Solutions Containing Volatile Weak Electrolytes*. AIChE Journal **21**, 1975, 248-259.
32. Edwards, T.J., Maurer, G., Newman, J. and Prausnitz, J.M., *Vapor-Liquid Equilibria in Multicomponent Aqueous Solution of Volatile Weak Electrolytes*. AIChE Journal **24**(6), 1978, 966-976.
33. Ellies A.J. and Golding R.M., *The Solubility of Carbon Dioxide Above 100°C in Water and in Sodium Chloride Solutions*. American Journal of Science **261**, 1963, 47-60.
34. Ellies, A.J., *The Effect of Pressure on the First Dissociation Constant of Carbonic Acid*. J. Chem. Society **750**, 1959, 3689-3699.
35. Glasscock, D. and Rochelle, G.T., *Numerical Simulation of Theories for Gas Absorption with Chemical Reaction*. AIChE Journal **35**(8), 1989, 1271-1281.
36. Glasscock, D., *Modeling and Experimental Study of Carbon Dioxide Absorption into Aqueous Alkanolamine*. Doctor of Philosophy Dissertation: The University of Texas at Austin Press, 1990.
37. Guggenheim, E.A., The *Specific Thermodynamic Properties of Aqueous Solutions of Strong Electrolytes*. Philosophical Magazine **19**(127), 1935, 588-643.
38. Harned, H.S. and Owen, B.B., *The Physical Chemistry of Electrolytic Solutions*. Reinhold Publishing, New York, 1958.
39. Harned, H.S. and Robinson, R.A., *Temperature Variation of the Ionization Constant of Weak Electrolytes*. Trans. Faraday Society **36**, 1940, 973-978.
40. Harned, H.S. and Scholes, S.R., *The Ionization Constant of HCO_3^- from 0 to 50°C*. Journal American Chemical Society **63**, 1941, 1706-1709.

41. Helgeson, C.H., *Silicate-Sea Water Equilibria in Ocean System*. Deep Sea Research and Oceanographic Abstract **17**(5), 1970, 877-892.
42. Hilliard, M.D., *Thermodynamics of Aqueous Piperazine/Potassium Carbonate/ Carbon Dioxide Characterized by the Electrolyte NRTL Model within ASPEN Plus 2004*. The University of Texas at Austin, 2004.
43. Othmer, K., *Encyclopedia of Chemical Technology*. Wiley, 2005.
44. Pitzer, R.M., Ermler, W.C., Winter, N., *An Algorithm for the Use of Symmetry in Molecular Self Consistent Field Calculations*. Chemical Physics Letter **19**, 1973, 179-182.
45. Posey, M.L., *Thermodynamic Model for Acid Gas Loaded Aqueous Alkanolamine Solutions*. Doctor of Philosophy Dissertation: The University of Texas at Austin, 1996.
46. Prausnitz, J.M., Lichtenthaler, R.N., de Azevedo, E.G., *Molecular Thermodynamics of Liquid Phase Equilibria,* Third Edition. Prentice Hall PTR: New York, 1999.
47. Rao, A.B. and E.S., Rubin, *A Technical, Economic, and Environmental Assessment of Amine Based Carbon Dioxide Capture Technology for Power Plant Greenhouse Gas Control*. Environment Science Technology **36**(20), 2002, 4467-4475.
48. Reddy, S., Johnson, D. and Gilmartin, D., *Fluor's Econamaine FG Plus Technology: An Enhanced Amine Based Carbon Dioxide Capture Process*. Presented in Second National Conference on Carbon Sequestration in Department of Energy of USA, May 5-8 (2003).
49. Renon, H. and Prausnitz, J.M., *Local Compositions in Thermodynamic Excess Functions for Liquid Mixtures*. AIChE Journal **14**(1), 1968, 135-144.
50. Sholeh, M., *Selection and Characterization of New Absorbents for Carbon Dioxide Capture*. Doctor of Philosophy Thesis: Norwegian University of Science and Technology in Trondheim, 2005.
51. Smith, J.M., van Ness, H.C. and Abbot, M.M., *Introduction to Chemical Engineering Thermodynamics*. Mc Graw Hill: New York, 1996.
52. Smith, W.R. and Missen. R.W., *Strategies for Solving the Chemical Equilibrium Problem and an Efficient Microcomputer Based Algorithm*. Canadian Journal of Chemical Engineering **66**(4), 1988, 591-598.
53. Steiner, J.G., *Natural Gas Sweetening and Effect of Declining Pressure*. Statoil Project: Norwegian University of Science and Technology, 2001.

54. Tosh, J.S., Field, J.H., Benson, H.E. and Haynes, W.P., *Equilibrium Study of The System Potassium Carbonate, Potassium Bicarbonate, Carbon Dioxide, and Water*. Bur. Mines. Rept. Invest. **5484**, 1959, 1-23

55. Weisenberger, S. and Schumpe, A., *Estimation of Gas Solubilities in Salt Solutions at Temperature from 273 K to 363 K*. AIChE Journal **42**(1), 1996, 298-300.

56. Wilson, G.M., *Vapor-Liquid Equilibrium XI: A New Expression for the Excess Free Energy of Mixing*. J. of American Chemical Society **86**(2), 1964, 127-130.

VITA

Yan Provinta Laksana was born in Banyuwangi, East Java Province, Indonesia on January 14, 1984. He entered Sepuluh Nopember Institute of Technology (ITS), Surabaya in the August, 2001 at Chemical Engineering Department through National University Student Entrance Examination (UMPTN). As part of institute cooperative program he involved field study at PT. Pupuk Kujang, Cikampek, West Java Provinces one of ammonia and urea fertilizer producer in Indonesia. At August, 2006 he graduated as Bachelor of Engineering and from January, 2007 started working as Junior Engineer in PT. Polyprima Karyareksa, Cilegon, Banten provinces. He was assigned as engineer in some petrochemical process such as reactor, distillation, vacuum separation, and compressor optimization. During his work he also followed some training for industrial application such as Distributed Control System (DCS) training by Honeywell, Boiler Process Training by Department of Industry Republic of Indonesia, and Waste Water Treatment by Nalco. Since June, 2008 he resigned from PT. Polyprima Karyareksa and worked as Process Engineer in PT. Klaras Pusaka International, an Engineering-Procurement-Construction-Commissioning (EPCC) company in Jakarta. He employed for Asian Petroleum Development (APD) together with PT. Pertamina and Serica Energy, Ltd in Glagah Kambuna Project to design production facility of natural gas exploration at North Sumatera. In October 2008, he was accepted as one of Republic of Türkiye Government Scholarship to continue Master Degree in Gebze Institute of Technology, Gebze.